Developmental Biology xxx (xxxx) xxx–xxx

Contents lists available at ScienceDirect

Developmental Biology

journal homepage: www.elsevier.com/locate/developmentalbiology

Twenty million years of evolution: The embryogenesis of four *Caenorhabditis* species are indistinguishable despite extensive genome divergence

Nadin Memar[a,b,*], Sabrina Schiemann[a,c], Christian Hennig[a], Daniel Findeis[a], Barbara Conradt[b,d], Ralf Schnabel[a]

[a] Institut für Genetik, TU Braunschweig, Braunschweig, Germany
[b] Zell- und Entwicklungsbiologie, LMU München, Martinsried, Germany
[c] Sars International Centre for Marine Molecular Biology, University of Bergen, Bergen, Norway
[d] Center for Integrated Protein Science Munich – CIPSM, Department Biology II, Ludwig-Maximilians-University Munich, Germany

ARTICLE INFO

Keywords:
Caenorhabditis species
Embryogenesis
Evolutionary developmental biology (evo-devo)
4D microscopy
Bioinformatics
Cell lineage
Signaling pathway

ABSTRACT

The four *Caenorhabditis species C. elegans, C. briggsae, C. remanei and C. brenneri* show more divergence at the genomic level than humans compared to mice (Stein et al., 2003; Cutter et al., 2006, 2008). However, the behavior and anatomy of these nematodes are very similar. We present a detailed analysis of the embryonic development of these species using 4D-microscopic analyses of embryos including lineage analysis, terminal differentiation patterns and bioinformatical quantifications of cell behavior. Further functional experiments support the notion that the early development of all four species depends on identical induction patterns. Based on our results, the embryonic development of all four *Caenorhabditis* species are nearly identical, suggesting that an apparently optimal program to construct the body plan of nematodes has been conserved for at least 20 million years. This contrasts the levels of divergence between the genomes and the protein orthologs of the *Caenorhabditis* species, which is comparable to the level of divergence between mouse and human. This indicates an intricate relationship between the structure of genomes and the morphology of animals.

1. Introduction

Traditionally, species and their phylogenetic relations were mainly defined by anatomical and developmental criteria. For very similar species, cross fertility is an additional criterion to define a species. Today, molecular criteria gain more and more importance in phylogeny. It was a long-term goal to derive the morphology of organisms from their molecular information. An interesting question is how much of the genome could directly reflect anatomy and the developmental processes of organisms. Nematodes, which feature an extremely conserved anatomy through twenty million of years of evolution, may thus be a good model system to understand a potential relation between genomes and developmental strategies and morphology. Of course, the development of species should be well understood to investigate a potential correlation between development and genomes, which can be more or less perfectly analyzed today. In 1983, John Sulston and co-workers published the embryonic cell lineage of *C. elegans* and showed that it is essentially invariant (Sulston et al., 1983). This characteristic made *C. elegans* a formidable system to address questions concerning developmental processes and considerable progress has been made in understanding the embryogenesis of the nematode. The most closely related nematodes to *C. elegans* are the members of the *Caenorhabditis* species; these include *C. briggsae, C. remanei* and *C. brenneri* (Cho et al., 2004; Kiontke et al., 2004; Kiontke and Fitch, 2005).

While all species were found in anthropogenic habitats like compost and garden soil, only *C. elegans* and *C. briggsae* were found side by side in one sample isolated in France (Barriere and Felix, 2005). The geographic distribution of the different species is also quite different, especially for *C. brenneri*, which unlike the others has not yet been found in Europe or North-America (Kiontke and Sudhaus, 2006). In terms of reproduction, *C. elegans and C. briggsae* are hermaphroditic, whereas *C. remanei* and *C. brenneri* are gonochoristic.

The nematodes *Caenorhabditis elegans* and *Caenorhabditis briggsae* are well studied model organisms (Stein et al., 2003; Zhao et al., 2008; Dolgin et al., 2008; Felix and Duveau, 2012). In terms of evolutionary distance, the most recent common ancestor of *C. elegans* and *C. briggsae* existed 20 million years ago (Stein et al., 2003;

* Corresponding author at: Zell- und Entwicklungsbiologie, LMU München, Martinsried, Germany.
E-mail address: memar@bio.lmu.de (N. Memar).

https://doi.org/10.1016/j.ydbio.2018.12.022
Received 7 October 2018; Received in revised form 18 December 2018; Accepted 20 December 2018

Cutter et al., 2006, Cutter, 2008). Forward and reverse genetic screens were performed in *C. elegans* and *C. briggsae* to identify genes important for developmental processes (Fraser et al., 2000; Gönczy et al., 2000; Kamath et al., 2003; Sonnichsen et al., 2005; Verster et al., 2014). In addition, several analyses contributed to the comparison and understanding of the genomic structures of *C. elegans* and *C. briggsae* (Stein et al., 2003; Cutter et al., 2006, 2008). In contrast to vertebrates, the *C. elegans* and *C. briggsae* genomes maintain the synteny of chromosomes (autosomes 95%, X chromosomes 97%). However, extensive (hundreds) rearrangements occurred within chromosomes, and it is unclear how this may have altered gene expression patterns. A considerable proportion of protein coding genes show rather low homology between *C. elegans* and *C. briggsae* (Stein et al., 2003; Hillier et al., 2007). Stein *et al.* identified a total of 12,000 orthologs corresponding to 62% and 65% of the *C. elegans* and *C. briggsae* genes, respectively. These orthologs have only a mean percent identity of 75% at the protein level, which is comparable to the level of divergence between mouse and human orthologs (Stein et al., 2003). Nevertheless, it was shown that conserved early embryonic genes from *C. briggsae* and *C. remanei* function in *C. elegans* consistent with underlying genetic compatibilities in development despite species separation. On the other hand, even human gene homologs were found to function in *C. elegans* (Coroian et al., 2006; Shaye and Greenwald, 2011; McDiarmid et al., 2018). Nonetheless, it may not really be surprising that hybrids derived from *C. briggsae* and *C. elegans* are not viable considering the large number of genes diversified in the two species (Baird and Yen, 2000). This diversification is also called developmental system drift (DSD) and discussed as a cause for speciation (True and Haag, 2001).

A comparison of the embryonic development of *C. elegans* with *C. briggsae* was already performed by Zhao *et al.* using automated cell lineaging (Zhao et al., 2008). The authors compared the positions of 27 cells at the 350-cell stage, the cell death pattern in the MS lineage and the cleavage timing of the P cell lineage. Based on their results they concluded that the developments of these two nematodes are remarkably similar. Using DIC 4D-microscopy (Differential interference contrast (DIC) 4D-microscopy) in combination with SIMI©BioCell for cell lineage analysis, we show here that the embryonic development of *C. elegans* and *C. briggsae* is indeed similar—as similar as two *C. elegans* embryos to each other. Furthermore, we show that the embryonic developments of *C. remanei* and *C. brenneri* are also comparable to the embryonic development of *C. elegans* or *C. briggsae*. We analyzed the embryos during different stages of their development and we compared the positioning of their cells through cell division and cell migration. We conclude from our results that there is not much difference among the four *Caenorhabditis* species in the positioning of cells through cell division and that in all four nematodes the cells perform cell focusing to reach the final position within their respective region. In addition, we analyzed the differentiation of tissues (pharynx, intestine, muscle) using antibody staining to confirm our lineage analysis data. From this we conclude that the tissues are composed of the same number of cells, indicating that the same cells differentiate into the same tissues in all four nematodes. In addition, ablation experiments indicate that the pattern of the early inductions are also maintained during evolution. Based on these results, we conclude that embryonic development in the *Caenorhabditis* species is a highly conserved process. These findings are solid fundament to search now for molecular mechanism underlying these different conserved aspects of development, such as early inductions or tissue development. This will allow to potentially link molecular processes and morphogenesis.

2. Background

2.1. C. elegans embryonic development

During the early *C. elegans* embryonic development, four cleavage rounds lead to five different somatic founder cells called AB, MS, E, C, D and the germ line precursor P_4, which is the posterior sister of the D blastomere. (Deppe et al., 1978; Sulston et al., 1983). The somatic founder cells generate distinct sets of somatic tissues and distinct regions during embryonic development. While the embryo is developing, 671 cells are generated of which 113 undergo programmed cell death. Most of the cells generated (389 cells) are descendants of the AB blastomere. These cells form 200 neurons and 40 supporting cells, 72 hypodermal cells and half of the pharynx (49 cells), the remaining 28 cells contribute to the body mesoderm and the alimentary tract (Sulston et al., 1983; Schnabel and Priess, 1997b). The AB blastomere features a very complex development. As shown by ablation experiments, at least five cell-cell interactions/inductions are needed to generate eight different descendants of the AB blastomere: ABala, ABalp, ABara, ABalp, ABpla, ABplp, ABpra and ABprp, referred to as the 8-AB blastomeres (Austin and Kimble, 1987; Priess and Thomson, 1987; Schnabel, 1991; Wood and Kershaw, 1991; Bowerman et al., 1992a; Hutter and Schnabel, 1994, 1995a; Schnabel and Priess, 1997b). These inductions induce binary switches establishing the identities of the 8-AB blastomeres. They depend on two signaling pathways, the Delta/Notch- and the Wnt-pathway (Sulston et al., 1983; Bowerman et al., 1992b).

During the 2-cell stage, the anterior somatic AB blastomere is polarized by the posterior P_1 germline precursor via a Wnt-signal (Hutter and Schnabel, 1995b; Thorpe et al., 1997; Park and Priess, 2003). Subsequently, AB divides first into ABa and ABp and only two min later (25 °C), P_1 divides into EMS and P_2 (Schneider and Bowerman, 2003; Nance, 2005). The P_2 blastomere generates a Delta/Notch-signal conferred by APX-1/GLP-1 in *C. elegans* that establishes in an anterior-posterior induction the posterior fate of ABp (Bowerman et al., 1992a, 1992b). ABa and ABp divide along the future left-right axis. All four descendants of ABa and ABp are still polarized due to the first anterior-posterior induction of the P_1 blastomere, which establishes the anterior posterior identities of the 8-AB descendants (ABala, ABalp, ABara, ABalp, ABpla, ABplp, ABpra and ABprp) (Hutter and Schnabel, 1995b).

The MS blastomere, the anterior daughter of the EMS blastomere, plays a central role by inducing the left-right identities of ABara and ABalp at the early 8-AB cell stage of the embryo (Priess et al., 1987; Priess and Thomson, 1987; Hutter and Schnabel, 1994; Mango et al., 1994). The Delta/Notch-signaling pathway plays again a key role during this axis specification (Marius Klangwart & Ralf Schnabel unpublished). The MS founder cell itself gives rise to mesodermal tissues (muscle, pharynx and neurons). The posterior daughter of EMS, the E founder cell, produces 20 intestinal cells (Sulston et al., 1983; Nance and Priess, 2002; Lee and Goldstein, 2003). The fate dichotomy of MS and E depends on an induction from P2 mediated by the Wnt/beta-catenin asymmetry pathway (Schierenberg, 1987; Sulston et al., 1983; Rocheleau et al., 1997; Kaletta et al., 1997; Nance and Priess, 2002; Lee and Goldstein, 2003; Maduro et al., 2005).

After this phase of early embryonic development, the embryo undergoes proliferation rounds, until the bean stage also called premorphogenetic stage (hereafter referred to as 256-AB cell stage) is reached.

During embryogenesis, a total of 113 cells are eliminated by programmed cell death. An additional 18 cells are programmed to die during post-embryonic development (Sulston and Horvitz, 1977; Sulston et al., 1983; Horvitz, 2003; Conradt et al., 2016). Due to the stereotyped lineage, the position of a cell death in the lineage (cell identity) is always identical; however, the position in the embryo shows the same variation as all other cells shortly before the premorphogenetic stage. The exact time point when each cell dies (e.g. cells die within a 5–10 min time window) and the cell death engulfment are variable (e. g. some dying cells are not always engulfed by the same cells) (Hoeppner et al., 2001). During the “first wave of cell death” in the *C. elegans* embryo (220 min after the cleavage of P_0/9th round of cell division), 14 cells undergo programmed cell death. Thirteen of

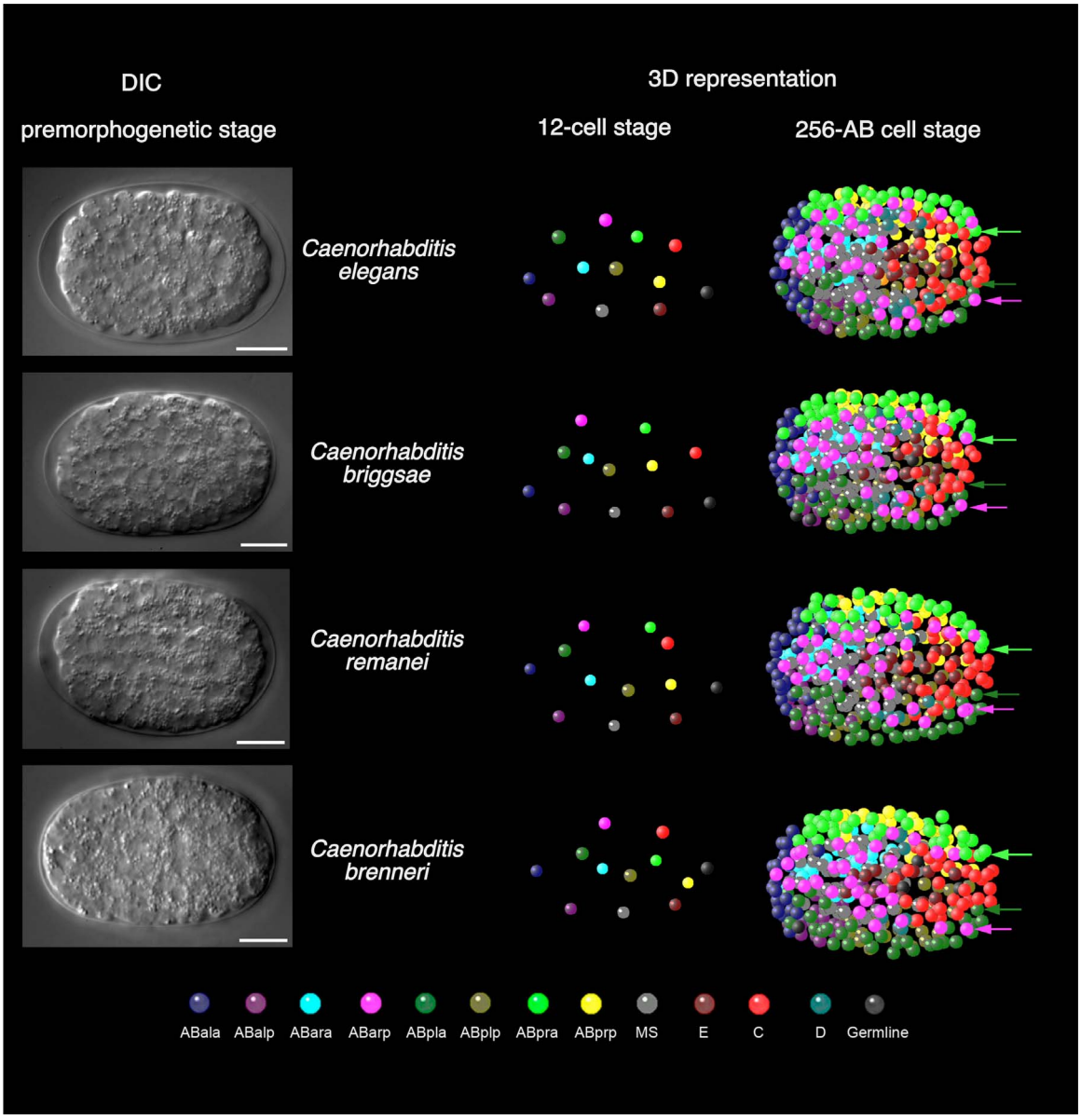

Fig. 1. Analysis of the 3D representations of *C. elegans*, *C. briggsae*, *C. remanei* and *C. brenneri* embryos (top to bottom). (**right**) DIC picture of the premorphogenetic stage (256-AB cell stage) of *C. elegans*, *C. briggsae*, *C. remanei* and *C. brenneri* wild-type embryos (scale bar 10 μm). (**left**) 3D representation of the *C. elegans*, *C. briggsae*, *C. remanei* and *C. brenneri* wild-type embryos at the 12-cell stage and at the 256-AB cell stage. All twelve color coded cells and their positions at the 12-cell stage are shown. Additionally, the position of their descendants (again color coded) is indicated in the 256-AB cell stage. The arrows are indicating specific cells at 256-AB cell stage (pink arrow ABarpppppp cell (V6R), dark green arrow ABplappppp (TL) and light green arrow ABprappppp (TR)).

these cells are AB descendants (4 in ABala, 2 in ABalp, 1 in ABara, 1 in ABarp, 0 in ABpla, 3 in ABplp, 0 in ABpra, 2 in ABprp) and one cell derives from MS (Sulston et al., 1983).

Since the cell death pattern is unique for a specific blastomere, it can be used to assign the fate of a particular founder cell or blastomere. An alternative way of analyzing the identity of a founder cell or blastomere is the positioning of its descendants at the 256-AB cell stage (Schnabel et al., 2006). During a process called “cell focusing” the cells navigate to their final position according to their fate (Bischoff and Schnabel, 2006; Schnabel et al., 2006). The descendants of the 8-AB blastomeres form discrete regions with specific shapes. For example, the descendants of ABarp form a Y-shaped region, in which each cell has a defined position. For example, ABarpppppp (V6R) is always positioned at the right end of the Y-shaped region (Bischoff and Schnabel, 2006; Schnabel et al., 2006) (see below; Fig. 1). Furthermore, at the 256-AB cell stage, the precursors of the different tissues, such as the pharynx cluster and the intestinal cluster, are already visible. Muscle and hypodermal cells, which surround the entire embryo, are also visible by Differential Interference Contrast (DIC) microscopy. Monoclonal antibodies can be used to detect these tissues and to quantify the number of cells in each tissue (Okamoto and Thomson, 1985; Priess and Thomson, 1987). After the 256-AB cell stage, the embryo elongates and the tissues complete their final differentiation. Once morphogenesis is completed, the L1 larva hatches.

2.2. Bioinformatic analysis

4D-microscopy and lineage analysis using the software SIMI©BioCell are ideal tools for analyzing embryonic development in different nematode species, with the high precision required to compare the embryogenesis of different species in order to quantify small differences (two embryos of each different species were analyzed, unless stated otherwise) (Fig. 1). Embryos show a natural variation of

size. Therefore, embryos have to be rescaled into a unit of measure. Because of this, the unit of measure "embryo length" (EL) was used. To make this unit comparable, all distances in an embryo were calculated as follows. All distances were normalized to the embryo length (EL) using the longest distance within an embryo. Afterwards, all embryos were scaled to 1 EL independently of their actual size.

Using 4D-microscopy and SIMI©BioCell, 4D-coordinates of the cells are collected with a precision of 0.5% embryo length (EL) on the x- or y-axis and 2% EL along the z-axis of the embryo, which is used for precise bioinformatic calculations (Material and Methods). The optical resolution of the DIC 4D-microscopy also enables an experienced user to identify cell fates i.e. tissues from the 256-AB cell stage onwards (Hutter and Schnabel, 1994; Schnabel et al., 1997a). Using SIMI©BioCell, we track the position of nuclei. Each nucleus has a defined coordinate (x,y,z), which reflects the general positions of cells up to the 256-AB cell stage since until this stage the nucleus is located in the center of the cell. After this stage, the nucleus can be asymmetrically located within the cell, especially in hypodermal and intestinal cells. Therefore, the 3D representations of the positions of nuclei reflect the arrangement of cells and thus the morphology of the embryo at a specific developmental stage up to the 256-AB cell stage (Figs. 1 and 2). The acquired cell coordinates can be used to create distance maps (Fig. 2). In distance maps, the distances of each cell to all other cells in the same embryo at a specific developmental stage is represented. For easier comparison, the calculated distance values are translated into a color code (RGB values) to visualize all cell distances among all cells (For example, the 32,640 distances (of a 256-AB cell stage embryo) at the premorphogenetic stage). Short distances are color coded in red (0–0.3 EL), medium distances in blue (0.3–0.7 EL) and long distances in green (0.7–1 EL). The rationale of the distance maps is depicted in Fig. 2. These distance maps are useful to directly compare the morphologies of different embryos directly. We feature two kinds of distance maps, the OX-distance map and the 3D-distance map. The OX-distance map only displays distance differences along the anterior-posterior axis (a-p), or the x-axis of the embryo (OX= Only X-axis map). This map disregards the two other axes (y, z). At first sight, the OX-map appears to be incorrect, but the representations are more clear than those produced by the 3D (x, y, z) maps (Fig. 6).

In order to compare the *Caenorhabditis* species, we need to be able to highlight very minor differences in the morphology of embryos, which can be hard to see by eye in a distance map. To be able to compare two embryos with each other and to highlight minor differences, two distance maps are subtracted to create the difference maps of these two embryos. The difference map represents the distance between two cells in one embryo compared to the distance between the same two cells in a second embryo. The values, which are calculated subtracting the RGB values of the two compared distance maps, are translated into a new color code. Small differences in distances are in black (0–0.3 EL), medium differences in distances are light blue (0.3–0.7 EL) and large differences in distances are yellow (0.7–1 EL) (Fig. 3). If cells have the same position in two different embryos at a specific developmental stage, their distance map values are the same. Thus, the subtraction of these values from each other will be 0% EL, which is represented by a black color. With increasing positional differences, the values are increasing up to 100% EL differences (Fig. 3). This allows the observer not only a quantitative but also regional appreciation of the morphological differences.

All quantifications span the 8-AB to the 256-AB cell stage and the sums for all values of all individual AB-derived cells existing during this period are considered. The RMS (root mean square) value describes the similarity/dissimilarity between two embryos at a specific developmental stage (Cohen et al., 1980; Schnabel et al., 2006). Two embryos with nearly identical cell positioning would have a RMS value close to zero. The highest dissimilarity between two embryos is reflected by a RMS value of 1. The comparison of two *C. elegans* embryos, which should have a nearly identical cell positioning, have a RMS of 0.042 at the 256-AB cell stage. To understand the similarity and dissimilarity of cell positioning of two embryos in more detail, we developed a vector based method, referred to AVD (Average Vector Dissimilarity), which also considers the alterations of directionality of cell positions. This

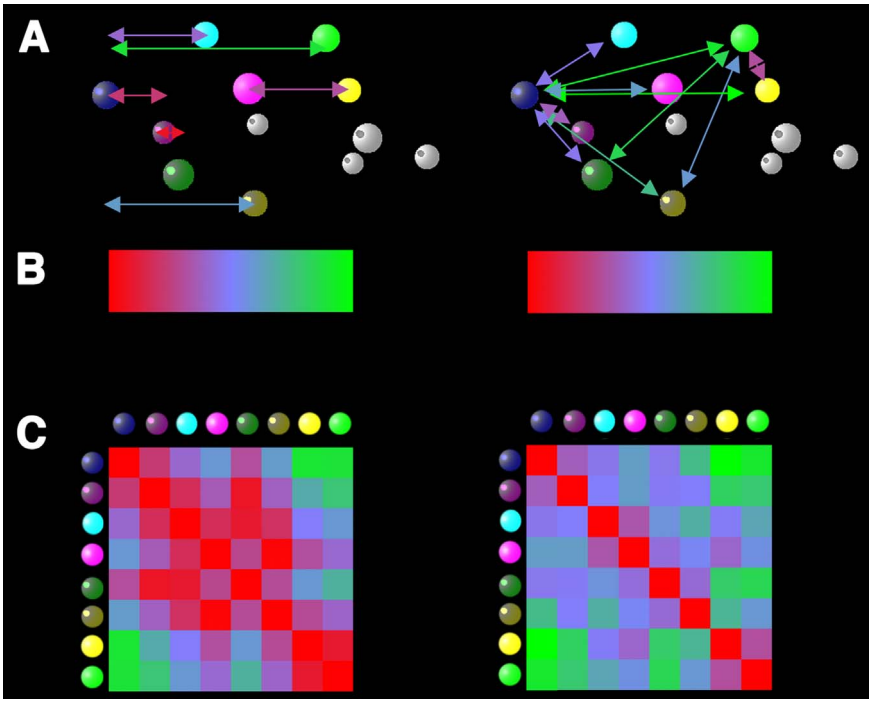

Fig. 2. The principle of distance maps (**A**) The eight AB derived blastomeres of the 12-cell stage embryo are used for clarity. We feature two kind of distance maps, the OX-distance map (left) and the 3D-map (right). The first is only displaying distance differences along the a-p, the x axis of the embryo. The second on the right is displaying distance differences in x,y,z-axis. The colors of the arrows represent the distances between cells. The colors correspond to the color code shown in (**B**), which represents all distances from 0% to 100% EL for both maps. (**C**) The matrices of the cells reflect all 64 combinations of the 8-AB cells present in the 12-cell stage embryo for the OX map (left) and the 3D map (right). The 64 blocks are colored according to the distance between the two specific cells, which results in a picture reflecting all distances among all cells and thus the morphology of the embryo.

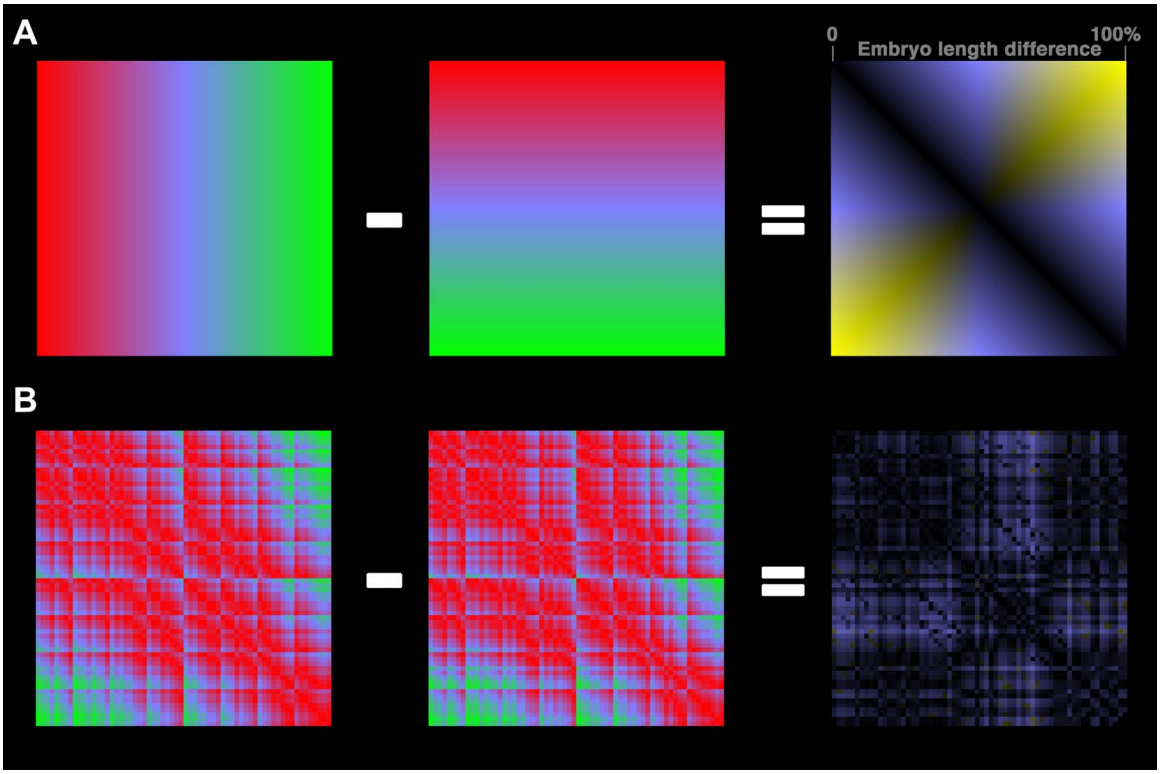

Fig. 3. The principle of difference maps. (**A**) Left, an artificial distance map created with the color code from red to green (left to right). Center, this map was turned 90 degrees, to generate a second map. Right, the two maps are subtracted. The result is an artificial difference map. A color gradient from black (0% EL) to bright blue for 50% EL. The following range to 100% EL difference is reflected by a gradient of yellow color. (**B**) Following this idea, the wild-type distance maps of two *C. elegans* 64-AB cell stage embryos were subtracted. The resulting difference map displays many blue and even yellow pixels (brightness enhanced with Photoshop value 75, for better visibility), indicating that cell positions vary significantly, up to 50% EL at mid embryogenesis to subsequently sort out in a much more conserved pattern (Fig. 5) (Schnabel et al., 2006, 1997a).

method reflects the dissimilarity of embryos in a linear function, which can be interpreted directly by the observer. This is an additional advantage of this method compared to the RMS-method.

One part of the bioinformatic analyses is the analysis of cell behavior. After a cell is born through cell division, the cell division gives the cell a specific position in the embryo. If we would only take in account the sum of all cell division (8-AB cell stage to the 256-AB cell stage), the cell would never reach its final position. The cells also need to migrate between the different cell division to reach their final position. For all cells in one embryo the sum of cell division, the sum of movement, the sum of effective migration (which reflects the linear connection of a cell after the position of the cell after cell division and the position before the cell divides further) can be calculated. Additionally, the division angle of all cells in one embryo can be calculated. Like the directionality of cell divisions, the transport of cells through cell divisions and cell migrations have been previously described for *C. elegans* (Schnabel et al., 2006).

3. Materials and methods

3.1. Nematode strains

Worms were grown at 25 °C as described (Brenner, 1974).

The following strains were used: *C. elegans* (N2 Bristol) (Brenner, 1974), *C. remanei* ssp. *vulgaris* (EM464) (Sudhaus, 1974; Baird et al., 1994), *C. briggsae* (AF16) (Fodor et al., 1983) isolation in Ahmedabad, India), C. *brenneri* (CB5161) (Isolated from sugar cane in Trinidad by D.J. Hunt (Commonwealth Institute of Parasitology) (Kiontke and Sudhaus, 2006).

3.2. 4D-microscopy

The method for 4D-microscopy was described previously (Schnabel et al., 1997a). Modifications of this system are described in Schnabel et al. (2006). All recordings were acquired at 25 °C. For *C. remanei* and *C. brenneri* a red filter was used, since embryos of these species are sensitive to white light.

3.3. Lineage analysis

All 4D-recordings generated were analyzed using the Software Database SIMI©BioCell (SIMI Reality Motion Systems, Unterschleissheim, Germany; http://www.simi.com/) (Schnabel et al., 1997a, 2006; Bischoff and Schnabel, 2006). Cells are followed by the observer and the coordinates are recorded approximately every 2 min. The cell cleavages are assessed by marking the mother cell before the cleavage furrow ingresses and subsequently the centers of the daughter cells three frames later (105 s). By marking every cell during the complete embryonic development, the complete cell lineage of an embryo is generated. These data can be used to generate 3D representations of all nuclear positions at any given developmental stage.

3.4. Micromanipulation of embryos by laser ablation

The embryos were ablated with a laser microbeam as described previously (Sulston and White, 1980; Sulston et al., 1983; Schnabel, 1991). The EMS cell was ablated after the division of P_1 was completed and the EMS nucleus was in the center of the cell. The energy of the laser beam was checked for each ablation by measuring the diameter of a hole burned into a coverslip. The ablation time was adapted to the nematode strain analyzed. For example, *C. briggsae* (ablation time ~3 min 30 s) was less sensitive to the ablation than *C. remanei* (~ 1 min and 45 s) or *C. brenneri* (~2 min 15 s). In *C. elegans,* the EMS blastomere was ablated for 2 min and 30 s.

After ablations, all embryos were recorded with the 4D-microscope

and analyzed using the Software Database SIMI©BioCell. Embryos were scored as "successfully" ablated, when the blastomere did not divide or divided very much later than normally.

3.5. Immunofluorescence

L4 larvae were picked to NGM plates (ø 3,5 cm) with only a small inoculate of OP50. These worms were incubated at 25 °C over night. The next day, the worms and eggs were collected into a watch glass by brushing off the worms and eggs with a brush from the plate. The worms were cut using a scalpel to release the remaining eggs. After this, the eggs were mounted in a drop of water onto poly-L-Lysine hydrobromide (Sigma#P1524) coated multiwell slides (Medco). The Teflon coated slides have a height of ~25 µm corresponding to the height of an embryo. A cover slip (Menzel-Gläser 24x60 mm #1,5) was put on top. The slides were frozen on dry ice for 10 min. Before fixation, the cover slip was quickly removed and the slide incubated in 100% ice cold methanol (5 min) followed by 100% ice cold acetone (5 min). The slides were dried, until the acetone evaporated completely. The slides were then incubated for 15 min in 1xTBST and the primary antibody was added. The incubation was carried out over night at 4 °C in a humid chamber. The following day, the primary antibody was removed and the slides were washed in 1xTBST for 15 min. Then, the secondary antibody (Cy3 goat anti mouse) was added to each well and the slide was incubated in a humid chamber for 2–4 h at room temperature. The slides were washed subsequently in 1xTBST for another 15 min. The remaining liquid was removed and a Mounting Medium was added to avoid bleaching of the sample. A cover slip (24x50) was added and sealed with nail polish. For microscopy we used Zeiss Axioplan microscopes equipped with Nomarski optics. We used markers for body wall muscles (antibody 5–6), pharyngeal muscles (antibody 3NB12) and the intestine (antibody ICB4). The antibody 5–6 detects all body wall muscle cells that are generated during embryogenesis. It specifically recognizes the myosinA protein, which is encoded by the gene *myo-3* in *C. elegans*, which is expected to be conserved in the other nematodes. Indeed, *C. elegans* MYO-3 protein shares 94% identity with *C. briggsae* MYO-3, 94% identity with *C. remanei* MYO-3, as well 94% identity with *C. brenneri* MYO-3 and even 50% identity to human MHY7. The antibody 3NB12 recognizes 21 pharyngeal muscle cells in *C. elegans*, seven of which are derived from the AB blastomere and 14 from the MS blastomere (Okamoto and Thomson, 1985). In addition, two neurons and two intestinal muscle cells are detected with this antibody (Priess and Thomson, 1987). The antibody ICB4 detects the intestine (Okamoto and Thomson, 1985; Kemphues et al., 1988). It recognizes an uncharacterized glycoprotein, which is present in *C. elegans* embryos on the membrane of 20 intestinal cells, two intestinal valve cells, three pharyngeal gland cells and six to eight interlabial neurons.

3.6. Bioinformatic methods

The calculations used in this work, were performed with the Software called "Phainothea" developed in the Laboratory of Ralf Schnabel. Some of the calculations were used before in other publications (Bischoff and Schnabel, 2006; Schnabel et al., 2006)

3.6.1. Scaling of embryos

Embryos show a natural variation of size. Therefore, embryos have to be rescaled into a unit of measure. Because of this, the unit of measure "embryo length" (EL) was used. To make this unit comparable, all distances in an embryo were calculated as follows. All distances were normalized into the embryo length (EL) using the longest distance within an embryo. Afterwards, all embryos were scaled to 1 EL independently of their actual size.

3.6.2. Distance calculation

The cell positioning is specified in a three-dimensional coordinate system. The unit pixel was used for the X- and Y-coordinates. For the Z-coordinates, the focal planes were used. Usually, a *C. elegans* embryo has a height of 25 µm, which equates to 10 pixels. The position of a cell A is defined as $A_{x,y,z}$ = 10,20,30, e.g. Ax is the position on the x-axis, Ay is the position on the y-axis and Az is the position in Z-coordinate. The distance in a three-dimensional space between two cells A and B were calculated as follows:

$$\overline{AB} = \sqrt{(A_x - B_x)^2 + (A_y - B_y)^2 + (A_z - B_z)^2}$$

3.6.3. Calculation of morphological differences with pairwise comparisons of embryos (RMS-method)

The "root mean square"-formula (RMS) was originally established to measure differences between protein structures using the distances between the atomic nuclei (Cohen and Sternberg, 1980). The method was modified by Franko Bignone to analyze cell positions in the *C. elegans* embryo (Bignone, 2001; Cohen and Sternberg, 1980)

All deviations between all cell-cell-distances are squared, added to each other and divided by the total number of cell pairs compared. The extraction of the root out of the calculated value (RMS score) quantifies the dissimilarity between two embryos. Since embryos have different sizes they are normalized as described earlier (see scaling of embryos above) before the RMS is calculated. The unit is embryo length per distance of cell pairs (EL/cell distance).

3.6.4. Calculation of morphological differences with pairwise comparisons of embryos (AVD-method)

We learned that the RMS-formula, using the absolute value of a distance, does not correctly assess all differences of cell positions in embryos. For example, a cell, which is displaced orthogonally to the reference cell to a position with the same distance to the reference cell, will not produce a signal for its movement. Therefore, we developed a vector based method, we call AVD (Average Vector Dissimilarity), which also considers the directionality of alterations of cell positions. The three dimensional vectors of all 32,640 cell-cell distances at the 256-AB cell stage are calculated in the two embryos to be compared. The vectors of all cell pairs are subtracted and the magnitude of the differences of cell positions is calculated from the resulting vectors. Finally, the calculated mean of all magnitudes is used as a unit of measure for the dissimilarity of the embryos. This method reflects the dissimilarity of embryos in a linear function, which can be interpreted directly by the observer, which we consider a further advantage of this method compared to the RMS-method.

$$AVD = \frac{\sum_{a=1}^{n-1}\sum_{b}^{n} a+1 \left| \begin{pmatrix} Cell_{a,b_x} \\ Cell_{a,b_y} \\ Cell_{a,b_z} \end{pmatrix}_{Ref} - \begin{pmatrix} Cell_{a,b_x} \\ Cell_{a,b_y} \\ Cell_{a,b_z} \end{pmatrix}_{Com} \right|}{\left(\frac{n*(n-1)}{2}\right)}$$

The AVD-method requires, however, an optimal rotation of the compared embryos into each other using an elaborate and time-consuming procedure by searching the minimal AVD value of incremental rotations of 2° in 180 steps.

The RMS-method reflects very small dissimilarities, typically found in the *Caenorhabditis* species in an almost linear fashion to values up to approximately 0.1. Therefore, we still use this method in this analysis. Increasingly larger dissimilarities are described by a curve leveling off asymptotically to a value of 0.24 representing a completely randomized 256-AB cell stage. The calculations for the sum of movement or sum of cell division were described before in (Schnabel et al., 2006). The sum of effective migrations is calculated by adding the distances of all bee lines between cells are born and divide again (Fig. 4).

3.6.5. Distance maps

The rationale of the distance map is depicted in Fig. 2. The eight AB

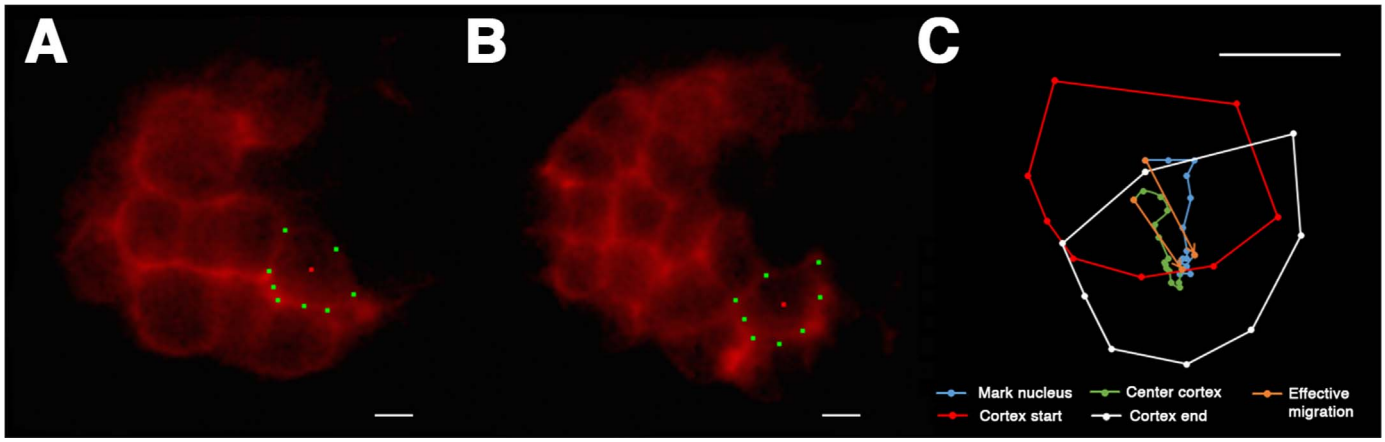

Fig. 4. Precision of the recording of cell position. (**A**) The cortex of the cell ABarapapp of an otherwise wild-type embryo is highlighted with a P*mex-5*::Lifeact::mKate2 transgene (SWG001) (Reymann et al., 2016) construct at the frame 175 of the recording. The green dots mark the shape of the cortex and the red dot the center of the cell, which we mark normally in the DIC recordings. (**B**) The end of the analysis of the cell at frame 188. The cell changes its shape constantly. (**C**) The red octagon represents the cortex at frame 175, the white octagon at frame 188. The eight positional marks are used to calculate the center of the cell, whose movement is shown by the 15 dots. The 15 dots show the marks of the visually tracked center. The corresponding marks deviate on average by 1.11 ± 0.53 µm (mean ± SD n = 15), which corresponds to 10% of the cell diameter at the 128-AB cell stage used for the analysis (scale bar 5 µm).

derived blastomeres of the 12-cell stage embryo are used for clarity. A matrix of 256 × 256 AB derived cells is used to create a distance map of the 256-AB cell stage (premorphogenetic embryo). The matrix reflects the order of cells in the lineage tree from anterior to posterior. Each single element in the matrix reflects the distance of two cells on the x-axis (Fig. 2A). The distance values range from 0 EL to 1 EL since at the 256-AB cell stage the AB descendants span the whole embryo. As explained earlier, the distance value 1 EL represents the longest distance between two cells in one embryo after scaling the embryo. For an easier comprehension, the calculated distance values are translated into the color code (RGB-values). The color code is a gradient from red across blue to green. Short distances are in red (0–0.3 EL), middle distances are blue (0.3–0.7 EL) and long distances are green (0.7–1 EL) (Fig. 3A and B) (Bignone, 2001; Bischoff and Schnabel, 2006; Schnabel et al., 2006)

3.6.6. Difference maps

The difference map represents the distance between two cells in one embryo compared to the distance between the same two cells in a second embryo. This representation is usually used to visualize deviations of a wild-type N2 embryo with a mutant embryo. In our studies, we use this method to compare wild-type embryos of different nematode species. The values, which are calculated subtracting the RGB values of the two compared distance maps, are translated into a new color code again. Short distances are in black (0–0.3 EL), middle distances are light blue (0.3–0.7 EL) and long distances are yellow (0.7–1 EL) (Fig. 3).

4. Results and discussion

4.1. The early cell positioning at the 12 cell stage is similar in all four Caenorhabditis species

The *C. elegans* 12-cell stage embryo represents the founder cell stage. In this stage, the 8-AB blastomeres are present and at the 256-AB cell stage their descendants form eight distinct regions in the *C. elegans* embryo (Fig. 1) (Sulston et al., 1983; Schnabel et al., 2006). We found that the early development of *C. briggsae*, *C. remanei* or *C. brenneri* are similar to that of *C. elegans* (Fig. 1). Specifically, the cell positions and cell cleavage patterns producing the 12-cell stage are similar among these *Caenorhabditis* species. Furthermore, the cell contacts are the same. For example, like in *C. elegans*, the MS cell is in close contact with ABara and ABalp in *C. briggsae, C. remanei* and *C. brenneri* (Fig. 1). This is a prerequisite for the early inductions to follow the same pattern as in *C. elegans*, a notion that will be addressed below.

4.2. Embryos of all four Caenorhabditis species embryos are similar at the 256-AB cell stage

The descendants derived from the eight AB founder cells (32 cells each) form eight distinct regions at the 256-AB cell stage. Each cell in these regions occupies a specific position and this shapes the characteristic form of each region. For example, the “pink” region formed by the 32 descendants of the ABarp founder cell always spans the entire embryo from anterior to posterior, forming a Y-shaped structure in which the V6R cell (hypodermal cell) is the most posterior cell on the right site of the region (Fig. 1 pink arrow) (Sulston et al., 1983). At the 256-AB cell stage, there is only little deviation in the position of a specific cell in the different *C. elegans* embryos. Other hypodermal cells are very good examples as well. The TR (ABprappppp) and TL (ABplappppp) cells are the most posterior cells in cell lineage tree of the ABpra founder cell and the ABpla founder cell (Sulston et al., 1983). These cells also mark the posterior end of their corresponding region (Fig. 1, dark green and light green arrow). While the position of the different regions is conserved in the different *Caenorhabditis* species, the position of specific cells, such as V6Ra , TR or TL at the posterior end of their respective region is also conserved. In conclusion, the 3D-representations of *C. briggsae, C. remanei* or *C. brenneri* embryos are almost indistinguishable from that of *C. elegans* embryos at the 256-AB cell stage (Fig. 1).

4.3. The cell-cell distances are nearly the same in all four Caenorhabditis species

Next, we used different bioinformatic tools to analyze the similarities of the 256-AB cell stages in more detail. A 3D-representation does not allow to deduce the exact arrangement of cells in embryos, which is required to detect subtle differences among the *Caenorhabditis* species. However, this can be achieved using a distance map displaying all distances of cells in an embryo to all other cells in that embryo. All distance maps shown here represent the 256-AB cell stage. The matrices shown in Fig. 5, represent all AB descendants at the 256-AB cell stage of one particular embryo and therefore 36,400 (i.e. 256×256) distances (Bischoff and Schnabel, 2006; Schnabel et al., 2006). The cell-cell distances, which are the basis of these maps, can

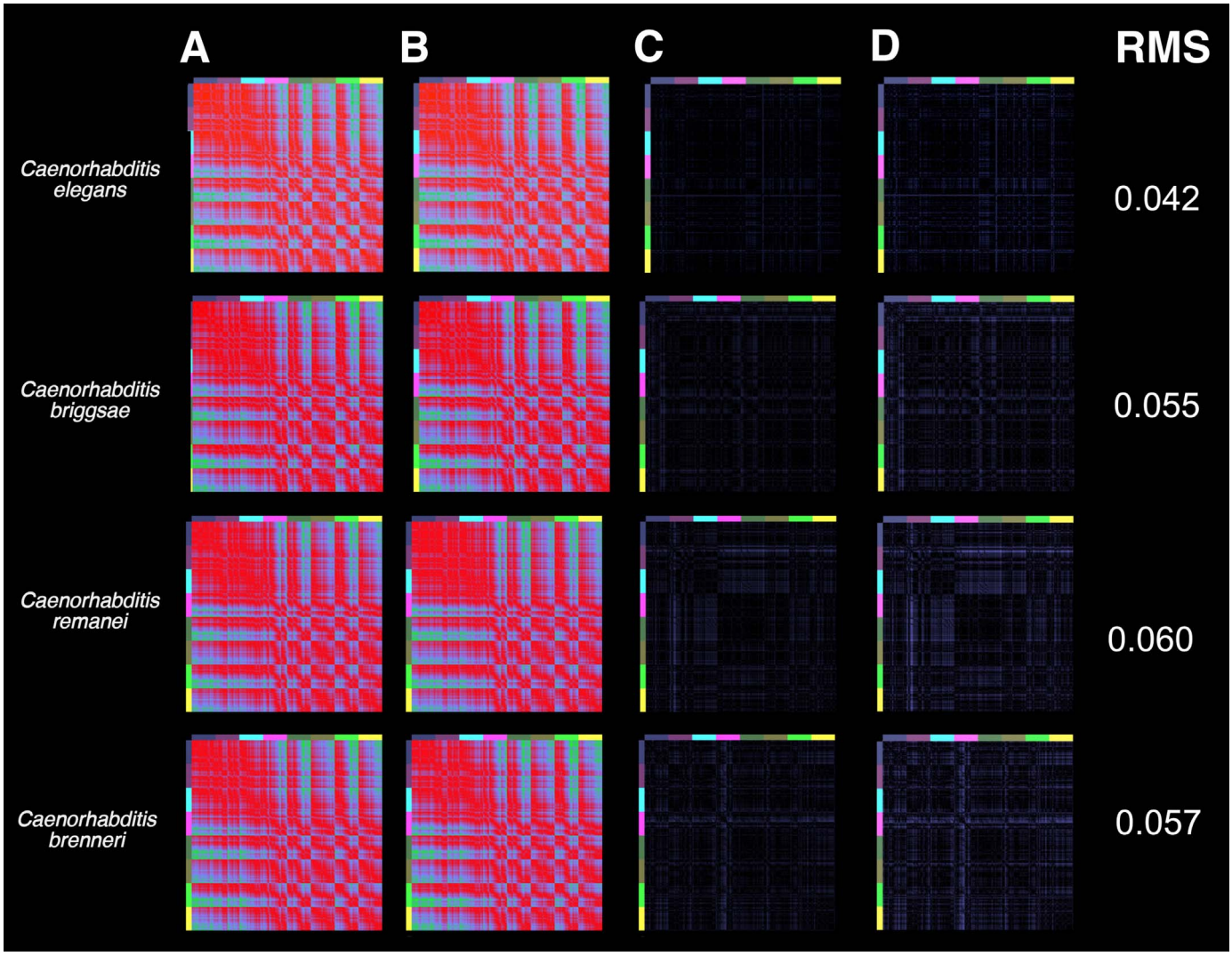

Fig. 5. Distance maps comparing cell positioning in embryos of two embryos of each species. (**A, B**) OX-distance maps of two embryos of each species. See for more detail Fig. 3 for the rationale of the distance map. (**C**) Original OX-difference maps as calculated by *Phainothea*. The OX-difference maps represent the differences of cell positioning at the premorphogenetic stage of all 256-AB descendants at the premorphogenetic stages. (**D**) For better visibility the brightness of the original OX-difference maps is enhanced by a value of 75 using Photoshop. The RMS is indicated, which describes the similarity/dissimilarity between two embryos at a specific developmental stage (Cohen et al., 1980; Schnabel et al., 2006).

also be used for a quantification of the similarity/dissimilarity of embryos using the RMS-Method (Fig. 5). We feature two kind of distance maps, the OX-distance map (Fig. 5) and the 3D-distance map (Fig. 6). The visual inspection of OX-distance maps of two embryos from each of the four *Caenorhabditis* species reveals almost no, if any, only subtle differences between the embryos of the same species and even among embryos of the different species. This suggest a conserved arrangement of cells and thus a conserved morphology of the embryos (Fig. 5A and B).

4.4. Subtle differences can be detected by comparing the four different species

To highlight the similarities and differences, we generated difference maps (see also Material and Methods and Fig. 3), a new bioinformatic approach, which permits the detection of even subtle differences in the morphology of embryos. With this method the distance maps of two *C. elegans* embryos were subtracted (Fig. 5C). The resulting difference map is almost, but not entirely black, which shows the sensitivity of our method, as subtle differences are detected. The resulting difference maps of the remaining three species are also almost entirely black; however, more and slightly brighter blue pixels are visible as well. To enhance the differences of the maps, their brightness was increased in Fig. 5D; however, only the colors in Fig. 5C represent the real colored differences. Inspection of the distance maps shows that the embryogenesis of *C. remanei* and *C. brenneri* are more variable than those of *C. elegans* or *C. briggsae*. However, we consider this to be due to statistical fluctuation, since the quantitative analysis presented below shows that the morphological variability of the *C. remanei* and *C. brenneri* embryos is not greater than that of 10 analyzed *C. elegans* embryos.

After analyzing the variability of the morphology in the same species, we generated 3D-distance and 3D-difference maps. These maps are used to compare the different species with each other (Fig. 6). Due to the higher sensitivity of the 3D- versus the OX-distance map, a careful visual inspection reveals additional, but still subtle differences in the maps of the four species. In all difference maps (except those from *C. brenneri*) subtle positional differences are distributed throughout the entire AB lineage. The difference maps of *C. brenneri* with all other species show in addition a light blue “cross”, which is caused by the fact that the Y-shaped region formed by the descendants of ABarp appears less organized in *C. brenneri* than in the other nematodes. The identification of subtle differences demonstrates the high sensitivity of the method. This analysis shows that the morphology of the 256-AB cell stage is similar in the

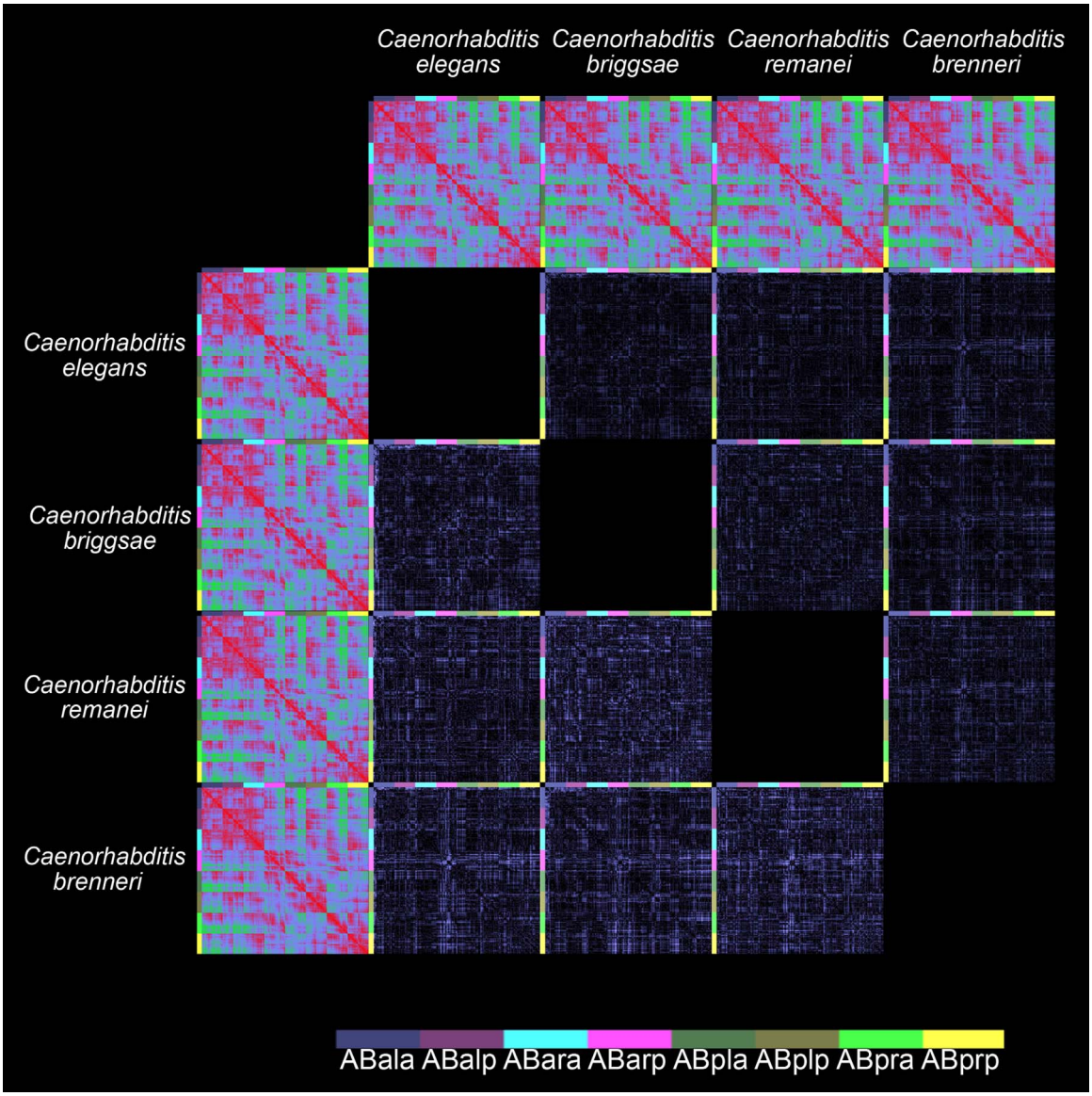

Fig. 6. 3D-difference maps of all members of the *C. elegans* species. The figure shows a matrix of 3D-distance maps embryos of the four *Caenorhabditis* species to display the 3D-difference maps of all possible combinations of the embryos. As in Fig. 5D, the brightness of the original difference maps is enhanced by a value of 75 using Photoshop.

analyzed *Caenorhabditis* species. As shown below, this is also true for the terminal fates of cells.

4.5. At the 256-AB cell stage, the variability of the four Caenorhabditis species is similar to the variability among ten C. elegans embryos

The root mean square (RMS) value describes the similarity/dissimilarity between two embryos at a specific developmental stage (Cohen et al., 1980; Schnabel et al., 2006). The two *C. elegans* embryos shown in Fig. 5 have an RMS value of 0.042 at the 256-AB cell stage. The RMS values for the three other species range from 0.055 to 0.06 (Table 1), which reflects as expected the brightness of OX-Difference-maps (Fig. 5). The RMS values of the comparison of the different species with all other species range from 0.053 to 0.063 reflecting also the brightness of the 3D-Difference-maps (Table 1, Fig. 6). The RMS values of a large sample of ten *C. elegans* embryos range from 0.045 to 0.083. Therefore, the variabilities of the 256-AB cell stages of the *Caenorhabditis* species investigated here fall within the range of variability observed among several *C. elegans* embryos. We conclude that the embryos of the four *Caenorhabditis* species are similar.

4.6. Cell division, cell migration and cell focusing are needed to position the cells in all four Caenorhabditis species

The descendants of the 8-AB blastomeres need to reach their positions in the body plan according to their fate in order to form a viable larva. For this to occur, cells need to divide, move and sort to their terminal position. The sorting process, which is coupled to far-ranging cell movements, was initially described for *C. elegans* (Cohen et al., 1980; Schnabel et al., 2006) and termed "cell focusing". The average directions of the cell divisions are very similar in the species ranging from 36.80° to 43.90° relative to the a-p axis. The total transport of cells by cell divisions varies in the species from 33.1 EL to 35.8 EL, with the exception of *C. remanei,* which has a total transport though cell division of 40.3 EL. The sum of movements of all cells (excluding the transport through cell divisions), varies in the species from 90.4 EL to 109.75 EL, with the exception of *C. remanei,* which has a total movement of 139,05 EL (Table 2). Lastly, we calculated the effective migration, which reflects the sum of the distances between the positions, at which the cells are born and at which they divide again. The sum of all effective migrations is 43.35 EL or 43.05 EL for *C. elegans* and *C. brenneri*, respectively and 53.6 EL or 56.15 EL for *C. briggsae* and *C. remanei*, respectively

Table 1
RMS values for the comparison of the morphologies of the four *Caenorhabditis* species.

Norm	z scale		*C. elegans* Consensus	*C. elegans* IB	*C. briggsae*	*C. remanei*	*C. brenneri*
490	13	***C. elegans* IB**	0,035	x	0,056	0,053	0,062
470	13	***C. briggsae***	0,049	0,056	x	0,055	0,062
490	13	***C. remanei***	0,051	0,053	0,055	x	0,063
484	12	***C. brenneri***	0,052	0,062	0,062	0,063	x
494	14	***IB Only mitoses***	0.166	0.169	0.169	0.174	0.164

The Root-Mean-Square-Method quantifies the similarity/dissimilarity of embryos as described previously (Bischoff and Schnabel, 2006; Schnabel et al., 2006). See for more detail the Materials and Methods. The *C. elegans* consensus is an embryo in which cell positions correspond to the mean positions calculated from ten normal N2 embryos. The RMS values for a N2 embryo IB "only mitoses" in which all cell movements are removed bioinformatically. The high RMS values indicate that cells are normally sorted in the body plan by cell migration, i.e. cell focusing. (Norm) Longest distance between cells in the embryo. (z scale) Number of z-stacks, recorded every 35 s, from the 12-cell stage to the 256-AB cell stage.

Table 2
Analysis of cell behavior during development.

	Norm	*z scale*	*frames*	*Sum of movement*	*Sum of effective migration*	*Sum of mitosis*	*average division angle (daughter -daughter) a-p*	*SD*	*average division angle (mother -daughter)a-p*	*SD*
C. elegans IB	490	13	362	96.80	44.10	36.70	33.6	20,3	37.8.	20.9
C. elegans AW	476	13	314	84.00	42.60	29.50	30.9	20,3	35.8.	22.3
C. elegans average				90.40 ± 9.05	43.35 ± 1.06	33.10 ± 5.09	32.25	20.30	36.80	21.60
C. briggsae 2	494	13	352	112.80	53.00	33.20	38.5	18.7	44.1	19.1
C. briggsae 3	470	13	293	106.70	53.60	38.40	34.9	20.3	40.1	21.7
C. briggsae average				109.75 ± 4.31	53.30 ± 0.42	35.80 ± 3.68	36.70	19.5	42.10	20,40
C. remanei 2	387	13	538	131.90	60.30	38.40	36.0	19.9	42.3	21.4
C. remanei 6	490	13	487	146.20	52.00	42.20	30.1	22.5	36.8	22.7
C. remanei average				139.05 ± 10.11	56.15 ± 5.87	40.30 ± 2.69	33.05	21.20	39.55	22.05
C. brenneri 3	444	12	566	100.00	42.70	36.70	38.1	19.8	45.3	21.1
C. brenneri 5	484	12	561	107.80	43.40	31.80	37.8	20.3	42.5	20.9
C. brenneri average				103.90 ± 5.52	43.05 ± 0.49	34.25 ± 3.46	37.95	20.05	43.90	21.00

All quantifications of cell behaviors span the 8-AB to the 256-AB cell stage. The sums for all values of all individual AB derived cells existing during this period are considered. With the exception of the cleavage angles of cells, the unit is embryo length (EL). The first three columns specify the parameters used for the normalization of the embryos required to compare the embryos. (Norm) Longest distance between cells in the embryo. (z scale) Number of z-stacks, recorded every 35 s, from the 12-cell stage to the 256-AB cell stage. (frames) The number of frames must be used to normalize the "Sum of effective migration" since cells move proportionally to the generation time.

(Table 2). Our results show that in all four *Caenorhabditis* species cell migrations contribute much more to cell positioning between the 8-AB cell stage and the 256-AB cell stage.

All *Caenorhabditis* species need to position their cells using cell focusing during their development. The RMS-formula, using the absolute value of a distance, does not correctly assess all differences of cell positioning in embryos. For example, a cell, which is displaced orthogonally to the reference cell to a position with the same distance to the reference cell, will not produce a signal for its movement. Therefore, a vector based method was developed, called AVD (Average Vector Dissimilarity) (for detailed information see Material and Methods). The AVD ranges from 0 for complete identity to 0.34 representing the dissimilarity between embryos, where cells are placed only by cell divisions. The AVD considers the directionality of alterations of cell positions. The AVD values are 0.078 or 0.093 for *C. elegans* and *C. briggsae,* respectively (Table 3). For *C. remanei* and *C. brenneri,* the AVD values are higher with values for *C. remanei* of 0.107 and for *C. brenneri* of 0.105. These results indicate that in all four *Caenorhabditis* species the cells need to focus and that in *C. brenneri* and *C. remanei* the sorting by cell focusing is more extensively used compared to *C. elegans and C. briggsae* at 25 °C.

Table 3
AVD (Average Vector Dissimilarity) for all *Caenorhabditis* species compared to the same species.

	C. elegans AW	*C. briggsae 3*	*C. remanei 6*	*C. brenneri 5*
C. elegans IB	0.078			
C. briggsae 2		0.093		
C. remanei 2			0.107	
C. brenneri 3				0.102

The AVD indicates the similarity and dissimilarity of cell positioning of two embryos, which also considers the alterations of directionality of cell positions.

4.7. The body wall muscles, pharyngeal muscles and the intestine are composed of the same number of cells in all four Caenorhabditis species

Since cell positions are essentially invariant in the embryos of the *Caenorhabditis* species, we wondered, whether tissues are also identical in terms of cell numbers and arrangement. To that end, we used antibodies marking body wall muscles, pharyngeal muscles or the intestine (Wood, 1988) (for details see Fig. 7). The muscle specific antibody recognizes 81 body wall muscle cells in the *C. elegans* embryo (Ardizzi and Epstein, 1987) and we counted the same number of body wall muscle cells in the other three *Caenorhabditis* species (Fig. 7A and B). The antibody specific for the pharynx recognizes 21 pharyngeal muscle cells in *C. elegans*, seven of which are derived from the AB blastomere and 14 from the MS blastomere (Priess and Thomson, 1987). In addition, two neurons and two intestinal muscle cells are detected with this antibody (Priess and Thomson, 1987). This antibody detects in all four *Caenorhabditis* species 21 pharyngeal muscle cells (Fig. 7A and B). The third antibody detects among other cells predominantly the intestine very early in development (Kemphues

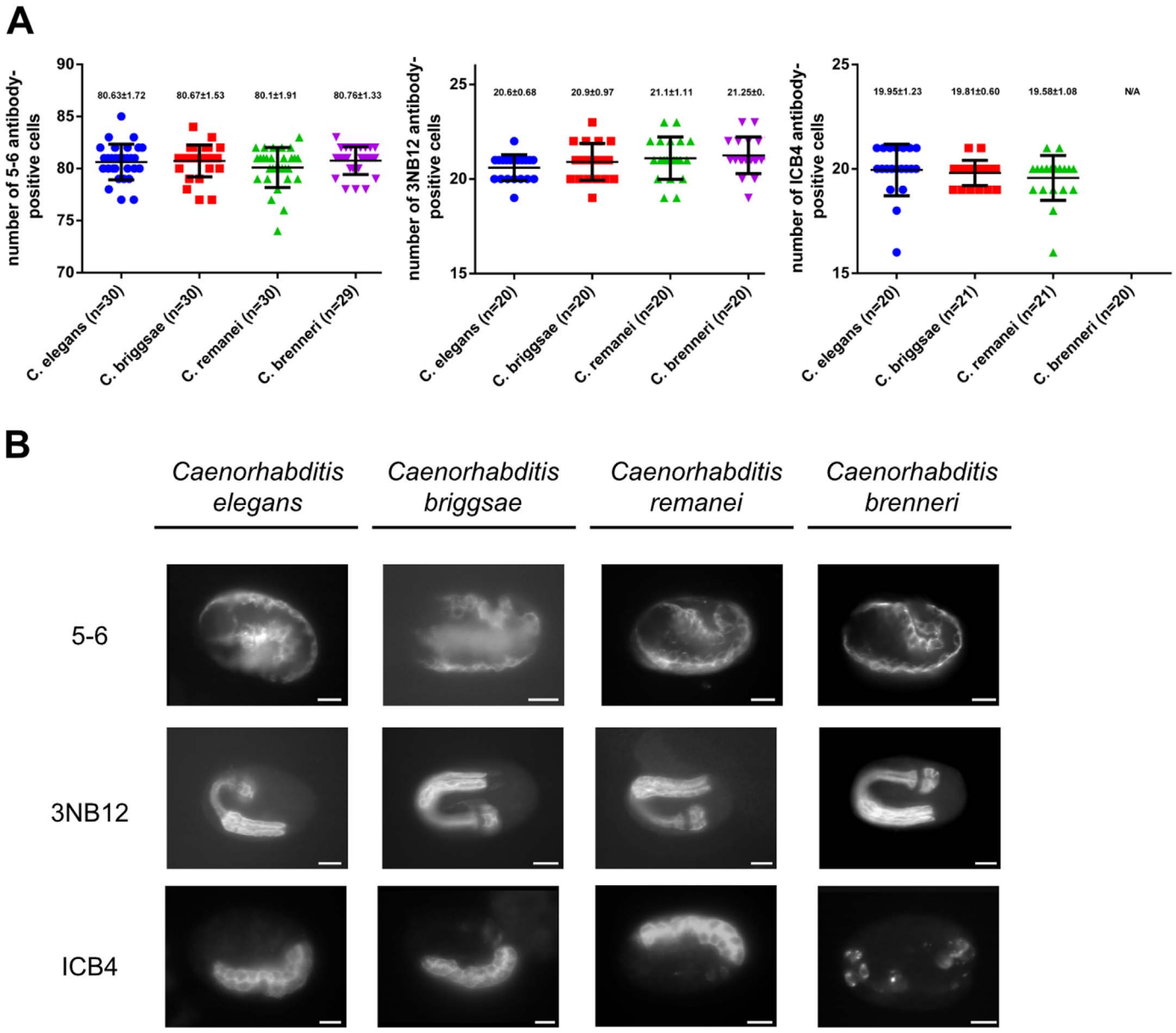

Fig. 7. Analysis of tissues by antibody staining. We used markers for body wall muscles (antibody 5–6), pharyngeal muscles (antibody 3NB12) and the intestine (antibody ICB4). The antibody 5–6 detects all body wall muscle cells that are generated during embryogenesis. (**A**) All four nematode species (*C. elegans, C. briggsae, C. remanei* and *C. brenneri*) were stained with these three antibodies and the cells detected were counted. With the antibody 5–6, we counted for *C. elegans* 80.63 ± 1.72 cells (mean ± SD, n = 30), *C. briggsae* 80.73 ± 1.53 cells (mean ± SD, n = 30), *C. remanei* 80.1 ± 1.91 cells (mean ± SD, n = 30) and *C. brenneri* 80.76 ± 1.33 cells (mean ± SD, n = 29). With the antibody 3NB12 detecting pharyngeal cells, we counted for *C. elegans* 20.6 ± 0.68 cells (mean ± SD, n = 20), *C. briggsae* 20.9 ± 0.97 cells (mean ± SD, n = 20), *C. remanei* 21.1 ± 1.11 cells (mean ± SD, n = 20) and *C. brenneri* 21.25 ± 0.97 cells (mean ± SD, n = 20). Finally, we counted intestinal cells detected by the ICB4 antibody in *C. elegans* 19.95 ± 1.23 cells (mean ± SD, n = 20), *C. briggsae* 19.81 ± 0.60 cells (mean ± SD, n = 21), *C. remanei* 19.58 ± 1.08 cells (mean ± SD, n = 21) and *C. brenneri* n/a. In *C. brenneri*, the staining was performed but no intestinal cells were stained (**B**) Representative images for each *Caenorhabditis* species stained with the antibodies used above (Scale bar 10 µm).

et al., 1988; Okamoto and Thomson, 1985). We counted on average 20 intestinal cells in *C. elegans, C. briggsae* and *C. remanei*. However, unfortunately, in *C. brenneri* the antibody did not detect intestinal cells, but some other structures. However, since the intestinal cells are detectable by DIC, the absence of staining is not due to the absence of intestinal cells, but probably to either the absence of the antigen in *C. brenneri* or to the divergence of the protein (Fig. 7A and B). Therefore, not only the positions of cells, but also the respective derived tissues are conserved in the *Caenorhabditis* species, indicating that in all four *Caenorhabditis* species the same cells contribute to the same tissues. Therefore, the conservation in the lineage translate into a conservation of cell fate. This is especially interesting because it was shown that while the embryonic lineage of *C. elegans* and the marine nematode *Pellioditis marina* are 95.5% conserved, interestingly 23.6% of the cell fates are different comparing these two nematodes (Houthoofd et al., 2003).

4.8. The early cell death pattern is kept during evolution but a difference can be seen in a later lineage

This motivated us to analyze the terminal fates of a comprehensive set of 41 cells in greater detail, including also cells from the P1 blastomere, which has so far not been analyzed in detail. 113 cells undergo programmed cell death during *C. elegans* embryogenesis (Sulston et al., 1983). All components (*egl-1*/BH3-only, *ced-9*/Bcl-2, *ced-4*/Apaf-1 *and ced-3*/Caspase) of the central apoptosis pathway identified in *C. elegans* can be found in C. *briggsae*, *C. remanei* and *C. brenneri* (Table 5A). Cell corpses can be easily detected during

Table 4
Cell fates in the *Caenorhabditis* species.

		Fate of the cells					
Cell name	***C. elegans***	***C. briggsae _2***	***C. briggsae _3***	***C. remanei _6***	***C. remanei _2***	***C. brenneri _3***	***C. brenneri _5***
ABala							
ABalaapapa	CD	CD	CD	CD	CD	CD	CD
ABalaappaa	CD	CD	CD	CD	CD	CD	CD
ABalapaaaa	N/CD	Cell lost	N/CD	N/CD	N/CD	N/CD	N/CD
ABalapapaa	CD	CD	CD	CD	CD	CD	CD
ABalappaaa	CD	CD	CD	CD	CD	CD	CD
ABalp							
ABalpaaaaap	P (m2VL)	P	P	P	P	P	P
ABalppaaaa	CD	CD	CD	CD	CD	CD	CD
ABalppaapa	CD	CD	CD	CD	CD	CD	CD
ABara							
ABaraaaaaaa	P (e1VL)	P	P	P	P	P	P
ABaraaaapp	CD	CD	CD	CD	CD	CD	CD
Abarappppp	N (IL2VR)	N	N	N	N	N	N
ABarp							
ABarpaaapp	CD	CD	CD	CD	CD	CD	CD
ABarpapppa	H (H0R)	H	H	H	H	H	H
ABarpapppp	H (H1R)	H	H	H	H	H	H
ABarppaaap	H (H2L)	H	H	H	H	H	H
ABarppappp	H (V6L)	H	H	H	H	H	H
Abarpppaap	H (H2R)	H	H	H	H	H	H
ABpla							
ABplaaaapa	H (hyp6)	H	H	H	H	H	H
Abplaaaapp	H (hyp6)	H	H	H	H	H	H
ABplaaapaa	H (XXXL;hyp)	H	H	H	H	H	H
ABplaaapap	H (hyp5)	H	H	H	H	H	H
ABplaaappa	H (HOL)	H	H	H	H	H	H
ABplaaappp	H (H1L)	H	H	H	H	H	H
ABplappppp	H (TL)	H	H	H	H	H	H
ABplp							
ABplppaaap	CD	CD	CD	CD	CD	CD	CD
ABplpppapp	CD	CD	CD	CD	CD	CD	CD
ABpra							
ABprappppp	H (TR)	H	H	H	H	H	H
ABprp							
ABprppaaap	CD	CD	CD	CD	CD	CD	CD
ABprpppapp	CD	CD	CD	CD	CD	CD	CD
ABprpppppppp	H/ hyp10	H	H	H	H	H	H
MS							
Msaaapaap	P (m4L)	P	P	P	P	P	P
MSaapapa	P/CD	P/P	P/P	cell lost	P/P	cell lost	P/ CD
MSpaapp	CD	CD	CD	CD	CD	CD	CD
MSpppapa	CD	CD	CD	CD	CD	CD	CD
MSpppapp	U	U	U	U	U	U	U
E							
Earaa	I	I	I	I	I	I	I
Eplppa	I/ intl8L	I/ intl8L	I/ intl8L	I/ intl8L	I/ intl8L	I/intl8L	I/intl8L
C							
Caaaaa	H/ hyp7	H	H	H	H	H	H
Caapap	CD	CD	CD	CD	CD	CD	CD
Cppaaap	U	U	U	U	U	U	U
D							
Daaaa	U	U	U	U	U	U	U
P							
P4a	Z3	Z3	Z3	Z3	Z3	Z3	Z3
P4p	Z2	Z2	Z2	Z2	Z2	Z2	Z2

List of cells lineaged further to assess their final fates during terminal embryogenesis. We analyzed two embryos of *C. briggsae*, *C. remanei* and *C. brenneri*. The cell fate was determined by using DIC microscopy and the lineage analysis, and cell positioning in the embryo (H= hypodermis, P = pharynx, CD= cell death, I=intestine, U=muscle, N = neuron, Z = germ line).

development due to their typical refractile (lense-like) morphology and the cell death pattern is characteristic for specific blastomere identities. Our lineage analysis indicates that in the four species, the cell death pattern is conserved like the development of the tissues (Figs. 1 and 7, Table 4). For example, during the 256-AB cell stage, four cell deaths occur in the ABala lineage in all species. In addition, we analyzed lineages with hypodermal, pharyngeal, body wall muscle, intestinal as well as neuronal fates to determine their terminal fate (Table 4). We could not identify significant differences among the four species. We could only find one fate alternation in two of the four species in the 41 analyzed cells (Table 4). In *C. elegans,* the MSaapapa cell gives rise to a pharyngeal cell and a cell death. We observed the same pattern in *C. brenneri* but not in *C. briggsae* or *C. remanei*. In these two species, the cell that dies in *C. elegans* and *C. brenneri*, survives and like its sister cell integrates into the pharynx. The conservation of the cell death pattern (with the exception of the MSaapapa cell) would suggest, that the activation of the cell death machinery at the appropriate time and place has been conserved as well. In summary, cell positions, the general tissue development and cell fates are conserved up to the 256-AB cell stage and were assessed even further.

Table 5
The protein homology of different pathway components.

A

	C. elegans	*C. briggsae*	*C. remanei*	*C. brenneri*
EGL-1 (BH3-only)				
C. elegans	100.00%	57.69%	57.84%	60.58%
C. briggsae	57.69%	100.00%	62.96%	65.42%
C. remanei	57.84%	62.96%	100.00%	58.88%
C. brenneri	60.58%	65.42%	58.88%	100.00%
CED-9 (BCL-2)				
C. elegans	100.00%	66.41%	60.53%	59.71%
C. briggsae	66.41%	100.00%	70.08%	68.94%
C. remanei	60.53%	70.08%	100.00%	62.22%
C. brenneri	59.71%	68.94%	62.22%	100.00%
CED-4 (Apaf-1)				
C. elegans	100.00%	81.28%	86.99%	71.81%
C. briggsae	81.28%	100.00%	88.47%	71.80%
C. remanei	86.99%	88.47%	100.00%	73.51%
C. brenneri	71.81%	71.80%	73.51%	100.00%
CED-3 (Caspase)				
C. elegans	100.00%	85.06%	84.66%	81.25%
C. briggsae	85.06%	100.00%	87.57%	86.00%
C. remanei	84.66%	87.57%	100.00%	84.20%
C. brenneri	81.25%	86.00%	84.20%	100.00%

B

GLP-1/LIN-12 (Notch)	*C. elegans glp-1*	*C. elegans lin-12*	*C. briggsae glp-1*	*C. remanei lin-12*	*C. brenneri lin-12*	*D. melanogaster Notch*
C. elegans glp-1	100.00%	48.95	56.41%	47.93%	47.20%	29.59%
C. elegans lin-12	48.95%	100.00%	47.86%	63.29%	62.64%	29.23%
C. briggsae glp-1	56.41%	47.86%	100.00%	45.91%	45.74%	28.83%
C. remanei lin12	47.93%	63.29%	45.91%	100.00%	58.93%	26.19%
C. brenneri lin-12	47.20%	62.64%	45.74%	58.93%	100.00%	28.43%
D. melanogaster Notch	29.59%	29.23%	28.83%	26.19%	28.43%	100.00%

C

APX-1 (Delta)	*C. elegans*	*C. briggsae*	*C. remanei*	*C. brenneri*	*D. melanogaster*
C. elegans	100.00%	57.55%	61.20%	54.24%	26.43%
C. briggsae	57.55%	100.00%	63.54%	53.91%	28.90%
C. remanei	61.20%	63.54%	100.00%	59.79%	25.36%
C. brenneri	54.24%	53.91%	59.79%	100.00%	27.49%
D. melanogaster	26.43%	28.90%	25.36%	27.49%	100%

The percent identity matrix of (**A**) EGL-1/BH3-only, CED-9/Bcl-2, CED-4/Apaf-1 and CED-3/Caspase protein (**B**) GLP-1/ Notchprotein and (**C**) APX-1/Delta of all four *Caenorhabditis* species was performed using Clustal2.1. The analysis was performed on protein sequences based on the homology indicated on www.wormbase.org.

4.9. The induction of the left-right symmetry depends on MS in all four Caenorhabditis species

Next, we investigated if the early inductions described for *C. elegans* are also conserved in the other species. As shown above, the 12-cell stage of the *Caenorhabditis* species is similar to the 12-cell stage of *C. elegans* (This is a stringent requirement for a similar induction pattern) (Fig. 1). The Delta/Notch-signaling pathway plays a key role in the induction by the MS blastomere of the left-right symmetry (l-r symmetry) during the 12-cell stage (Hutter and Schnabel, 1994). The most efficient way of testing the hypothesis that MS induces l-r asymmetries is laser irradiation of the EMS cell, the mother of MS. After this manipulation, the *C. elegans* embryo produces only four different l-r symmetric pairs of fates blastomeres (2x ABala, 2x ABarp, 2x ABpla, 2x ABprp). We determined the identity of each blastomere by analyzing the cell death pattern, since it is almost unique for each blastomere (Table 4). In the three other *Caenorhabditis* species (each n = 2), we scored the same altered cell death patterns after ablation of the EMS blastomere as we did in ablated *C. elegans* embryos (n = 2) (Hutter and Schnabel, 1995a, 1995b). For example, in untreated *C. elegans* embryos the ABara lineage normally executes one cell death (ABaraaaapp) whereas the ABala lineage executes four cell deaths (ABalaapapa, ABalaappaa, ABalapapaa and ABalappaaa). After ablation of EMS, ABaraaaapp does not die. Instead four other cells in that lineage die (ABaraapapa, ABaraappaa, ABarapapaa and ABarappaaa), which indicates a transformation of ABara into ABala. In all other *Caenorhabditis* species, we uncovered the same transformation of ABara into ABala after irradiation of EMS (Fig. 8). For the other blastomeres the expected cell fate changes upon EMS ablation could be observed (Fig. 8, Table 6).

Based on these findings we propose that the early l-r inductions depend on MS in all *Caenorhabditis* species and that their inhibition causes identical fate transformations. Of course, we cannot be certain that all *Caenorhabditis* species use Notch signaling for the l-r inductions (Priess et al., 1987); however, all genomes contain the corresponding genes (Table 5B and C). The similarities of the embryonic developmental patterns and even of the apparently conserved inductions do not necessarily indicate a detailed conservation of underlying developmental mechanisms. For example, the loss of *pop-1* function downstream of Wnt in E and MS development causes different phenotypes in *C. elegans* or *C. briggsae* (Owraghi et al., 2010). Furthermore, we can only speculate that the a-p induction, which is depend on Wnt signaling, (Schnabel and Priess, 1997b) is conserved as well, however, the observations of Owraghi et al. (2010) make this very likely.

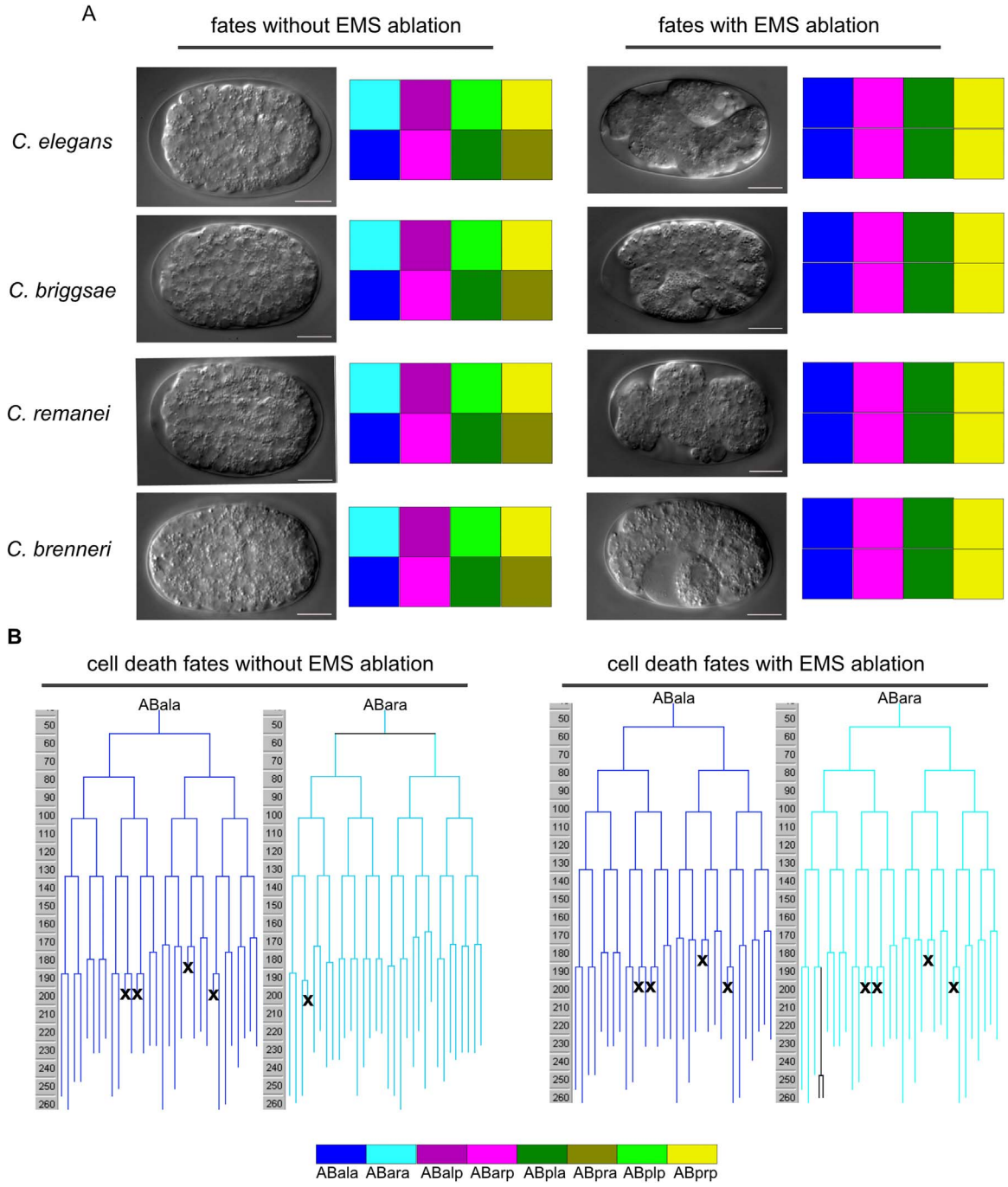

Fig. 8. EMS ablation. (**A**) The fates of the four *Caenorhabditis* species without ablation of the EMS cell and after ablation of the EMS cell are shown. The fates are color coded as before. Without ablation, the DIC pictures represent the 256-AB cell stage of *C. elegans, C. briggsae*, *C. remanei* and *C. brenneri*. The ablation of the EMS cell was performed in the 4-cell stage as described in the Material and Method section. The DIC pictures of the EMS ablation represent the terminal stage of each embryo analyzed. For each species two embryos were analyzed (scale bar 10 µm). (**B**) The cell death pattern in the ABala and ABara lineage before and after EMS ablation. The cell death pattern is indicated by black crosses. The cell fates are indicated by color code. An additional cell division due to cell fate changes is indicated in black. See for more detail also Table 6.

4.10. The developmental timing is different among the four Caenorhabditis species

As mentioned above, the developmental timing is not significantly different between *C. elegans* embryos provided that the embryos develop at the same temperature (Schnabel et al., 1997a). The early divisions are very rapid. For example, the AB blastomere, which gives rise to most of the somatic tissue, divides 2 min before the P_1 cell, which is the precursor of the germline (Brauchle et al., 2003). Until the fifth round of cell division, the cell cycle lengths are comparable in all nematodes. For example, the fourth cell cycle (ABar cell - ABarp cell) is ~14 min long in *C. elegans* and in *C. briggsae*. In *C. remanei* and *C. brenneri*, this cell cycle takes ~18 min, which is still in the same range. However, after the fourth cell cycle, a considerable change in the developmental timing of the four *Caenorhabditis* species occurs. In *C. elegans* and in *C. briggsae,* the cell cycles are continuously getting longer (Fig. 9A and B). The fourth cell cycle is 15 min long, the fifth and sixth cell cycle are 24 min long and the seventh cell cycle is already around 30 min long. In comparison, in *C. remanei* and *C. brenneri* the fourth cell cycle is 28 min long. The fifth cell cycle in *C. remanei* is 50 min long and even longer in *C. brenneri* with 75 min. There is a sudden increase in cell cycle length, which looks like a pause in

Table 6
Cell fates in the *Caenorhabditis* species after ablation of the EMS blastomere.

			C. elegans		*C. briggsae*		*C. remanei*		*C. brenneri*	
Cell name	***Fates in C. elegans according to*** Sulston (1983)	***Fates after EMS ablation according to*** Hutter and Schnabel (1994)	***8.8***	***15.7***	***#1***	***#3***	***#6***	***#5***	***#2***	***#4***
ABala	**ABala**	**ABala**								
ABalaapapa	CD	CD	CD	CD	CD	CD	CD	CD	CD	CD
ABalaappaa	CD	CD	CD	CD	CD	CD	CD	CD	CD	CD
ABalapapaa	CD	CD	CD	CD	CD	CD	Cell lost	CD	CD	CD
ABalappaaa	CD	CD	CD	CD	CD	CD	CD	CD	CD	CD
ABalp	**ABalp**	**ABarp**								
ABalpaaapp	Div	CD	CD	CD	CD	CD	CD	CD	CD	CD
ABalppaaaa	CD	H	H	H	H	H	H	H	H	H
ABalppaapa	CD	H	H	H	H	H	H	H	H	H
ABalppappp	Div	H	H	H	H	H	H	H	H	H
ABalpppaap	Div	H	H	H	H	H	H	H	H	H
ABara	**ABara**	**ABala**								
ABaraaaapp	CD	Div	Div	Div	Div	Div	Div	Div	Div	Div
ABaraapapa	Div	CD	CD	CD	CD	CD	CD	CD	CD	CD
ABaraappaa	Div	CD	CD	CD	CD	CD	CD	CD	CD	CD
ABarapapaa	Div	CD	CD	CD	CD	CD	CD	CD	CD	CD
ABarappaaa	Div	CD	CD	CD	CD	Cell lost	CD	CD	CD	CD
ABarp	**ABarp**	**ABarp**								
ABarpaaapp	CD	CD	CD	CD	CD	CD	CD	CD	CD	CD
ABarppaaaa	N	N	N	N	N	N	N	N	N	N
ABarppaapa	H	H	H	H	H	H	H	H	H	H
ABarppappp	H (V6L)	H	H	H	H	H	H	H	H	H
ABarpppaap	H (H2R)	H	H	H	H	H	H	H	H	H
ABpla	**ABpla**	**ABpla**								
ABplaaappp	H(H1L)	H	H	H	H	H	H	div	H	H
ABplp	**ABplp**	**ABprp**								
ABplpappap	CD	div	div	div	div	div	div	div	div	div
ABplpppapp	CD	CD	CD	CD	CD	CD	CD	CD	CD	CD
ABpra	**ABpra**	**ABpla**								
ABpraaappp	div	H	H	H	H	H	H	H	H	H
ABprp	**ABprp**	**ABprp**								
ABplpappap	div	div	div	div	div	div	div	div	div	div
ABprpppapp	CD	CD	CD	CD	CD	CD	CD	CD	CD	CD

List of cells lineaged further to assess their final fates during terminal embryogenesis. We analyzed two embryos each of *C. elegans*, *C. briggsae*, *C. remanei* and *C. brenneri* after ablation of the EMS cell. (H= hypodermis, CD= cell death, div= cell division).

development. After this, all cell cycles in these nematodes are approximately 60 min. *C. remanei* and *C. brenneri* need more time for the embryonic development than *C. elegans* and *C. briggsae* (Fig. 9B). Furthermore, the time to reach the 32-AB cell stage in the embryonic development of *C. brenneri* is twice as long as that in *C. elegans* and *C. briggsae*. The very pronounced differences in the timing of the developmental events have so far, no consequences for the other conserved processes.

5. Conclusion

After a hundred years of work on the embryogenesis of nematodes (see review by zur Strassen, 1959) the seminal lineage published by Sulston *et al.* appeared to support the old conclusion that nematodes are a major paradigm for a strictly determinate development (Sulston et al., 1983). As already discussed, a plethora of subsequent work suggested that most of the determination events depend on induction pathways also common in vertebrate development, which is considered paradigmatic for regulative (indeterminate) development. The inductions were masked till the late 1980ties by the stereotyped cleavage pattern in early development of *C. elegans*, which causes that always the same blastomeres are interacting during the inductions. This appears to be an event that occurred later on during nematode evolution, since nematodes positioned at the very base like *Tobrilus stefanskii* still show a regulative development without a stereotyped lineage (Schulze and Schierenberg, 2011). Thus, the general strategy to construct a nematode evolved considerably during evolution.

The phylogenetic divergence of the four *Caenorhabditis* species analyzed in this work has been estimated to date back over 20 million years (Stein et al., 2003; Cutter et al., 2006; Cutter et al., 2008). These long independent evolutionary histories have led to substantial genomic differences (Stein et al., 2003; Cutter et al., 2006; Cutter et al., 2008), yet the four species are highly similar in external morphology and, as far as known, in their habitat and ecological requirements (Barriere and Felix, 2005; Felix and Duveau, 2012). Because their distribution areas are largely non-overlapping (Kiontke and Sudhaus, 2006), this pattern would suggest an origin by allopatric, non-adaptive speciation. As discussed by True et al, this could occur just on the basis of a genetic drift (DSD) (True and Haag, 2001). However, the co-occurrence of *C. brenneri* in the same area as another member of the genus (*C. elegans*, *C. briggsae* and *C. remanei*) would also agree with an adaptive species formation under at least partly sympatric conditions, driven by a yet-to-be-discovered subtle adaptive (ecological) differentiation.

Ultimately, to decipher whether *Caenorhabditis* species formation was adaptive or non-adaptive will require integrating genomic data with in-depth studies of their ecology and natural history. With the data at hand, it appears to be most astonishing that these organisms are apparently characterized by a high substitution rate (Cutter, 2008), genome reductions related to different reproductive modes (Fierst et al., 2015) and a low protein level genomic identity comparable to that between human and mouse (Gupta and Sternberg, 2003). On the other hand, the four nematodes are extremely conserved in morphology and, as demonstrated herein, in almost every detail of their embryonic development. Additionally, all four *Caenorhabditis* species are polyclonal in their fate specification (i.e. cells, which form a

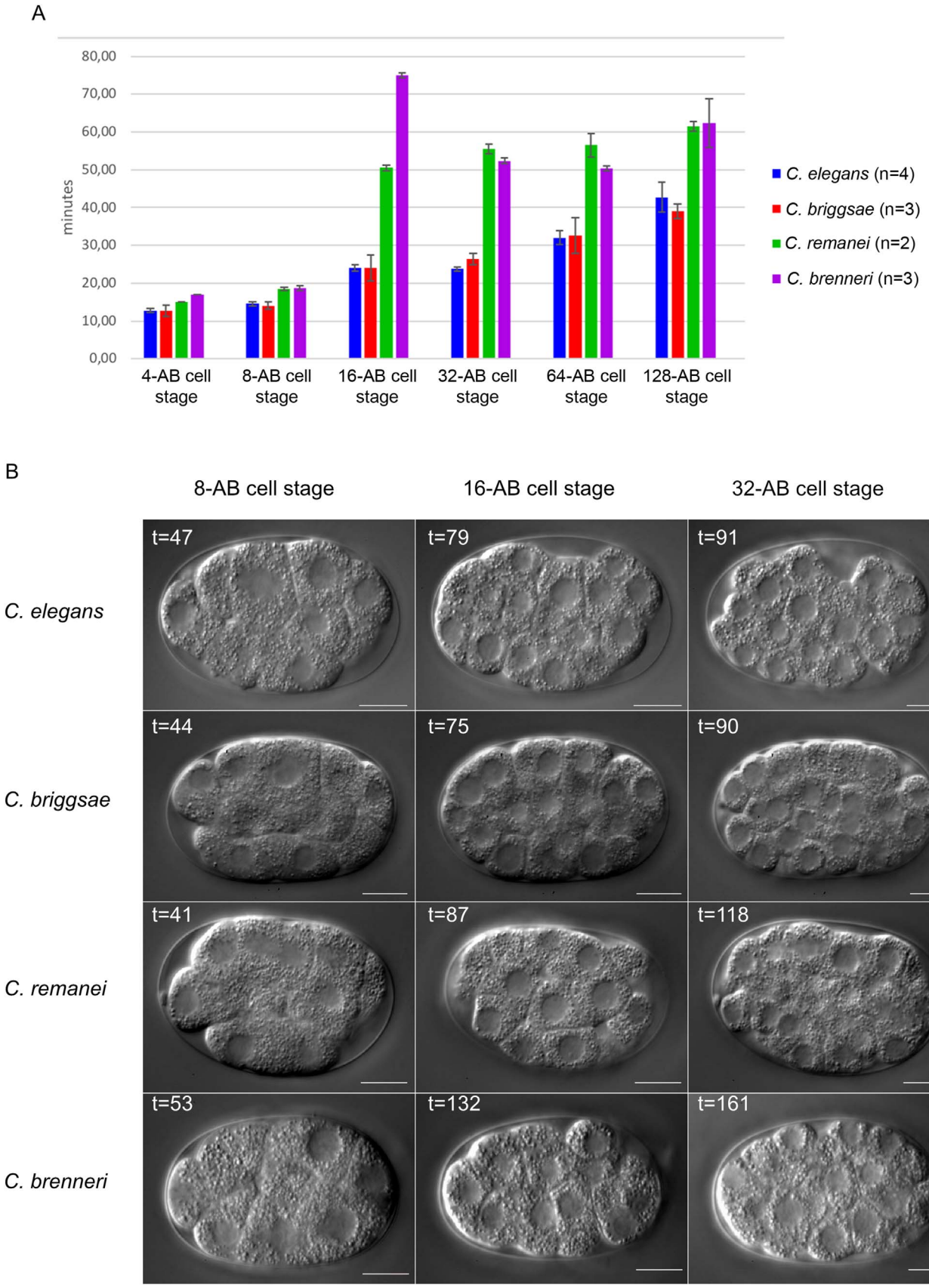

Fig. 9. Cell cycle length. (**A**) The cell cycle was measured for the ABarppppp lineage. ABarppppp is differentiating into the V6R hypodermal cell. The analysis was performed in *C. elegans* (n = 4), *C. briggsae* (n = 3), *C. remanei* (n = 2) and *C. brenneri* (n = 3). (**B**) DIC representation of all four analyzed nematodes at a specific developmental stage are shown: 8-, 16- and 32-AB cell stage the time (t) is in minutes (scale bar 10 μm).

particular tissue, derive from different lineages), which could explain the importance of cell focusing in these nematodes. In contrast, *Halicephalobus sp*. has a monoclonal lineage pattern and it was shown that in this nematode some cells need to migrate long distances to reach their final positions (Houthoofd et al., 2003). If these migrations are an exception or if the sum of all cell migrations is smaller or larger compared to the one of polyclonal cell lineages in *Caenorhabditis* species remains to be determined and needs to be analyzed with regard to advantage for embryonic development.

Classically, two not exclusive forces are discussed, which could be responsible to maintain the morphology i.e. the body plans of organisms or even in clades. The first is enormous selective pressure and the second a rigid developmental constraint acting to conserve morphology and development in these species for over 20 million years in the background of rather volatile genomes. However, in a new synthesis Vermeij et al argues that impediments to phenotypic evolution are often attributed to developmental constraints, are anyway due to selection, which decides what works and what does not work (Vermeij, 2015).

Acknowledgment

We thank Miguel Vences, Frank Döring and Stephane Rolland for helpful comments on the manuscript. Cathrin Struck, Nadja Lebedeva und Linda Jocham for the perfect technical assistance. Katharina Luthe for helping with lineaging. All current and past members of the Schnabel and Conradt group for the helpful discussions. Some strains were provided by the CGC, which is funded by NIH Office of Research Infrastructure Programs (P40 OD010440). This work was supported by the Deutsche Forschungsgemeinschaft (CIPSM; EXC114).

References

Ardizzi, J.P., Epstein, H.F., 1987. Immunochemical localization of myosin heavy chain isoforms and paramyosin in developmentally and structurally diverse muscle cell types of the nematode *Caenorhabditis elegans*. J. Cell Biol. 105, 2763–2770.

Austin, J., Kimble, J., 1987. *glp-1* is required in the germ line for regulation of the decision between mitosis and meiosis in *C. elegans*. Cell 51, 589–599.

Baird, S.E., Yen, W.C., 2000. Reproductive isolation in *Caenorhabditis*: terminal phenotypes of hybrid embryos. Evol. Dev. 2, 9–15.

Baird, S.E., Fitch, D.H.A., Emmons, S.W., 1994. *Caenorhabditis vulgaris* sp.n. (Nematoda: Rhabditidae): a necromenic associate of pill bugs and snails. Nematologica 40, 11.

Barriere, A., Felix, M.A., 2005. Natural variation and population genetics of *Caenorhabditis elegans*. WormBook, 1–19.

Bignone, F.A., 2001. Structural complexity of early embryos: a study on the nematode *Caenorhabditis elegans*. J. Biol. Phys. 27, 257–283.

Bischoff, M., Schnabel, R., 2006. Global cell sorting is mediated by local cell-cell interactions in the *C. elegans* embryo. Dev. Biol. 294, 432–444.

Bowerman, B., Eaton, B.A., Priess, J.R., 1992a. *skn-1*, a maternally expressed gene required to specify the fate of ventral blastomeres in the early *C. elegans* embryo. Cell 68, 1061–1075.

Bowerman, B., Tax, F.E., Thomas, J.H., Priess, J.R., 1992b. Cell interactions involved in development of the bilaterally symmetrical intestinal valve cells during embryogenesis in *Caenorhabditis elegans*. Development 116, 1113–1122.

Brauchle, M., Baumer, K., Gönczy, P., 2003. Differential activation of the DNA replication checkpoint contributes to asynchrony of cell division in *C. elegans* embryos. Curr. Biol. 13, 819–827.

Brenner, S., 1974. The genetics of *Caenorhabditis elegans*. Genetics 77, 71–94.

Cho, S., Jin, S.W., Cohen, A., Ellis, R.E., 2004. A phylogeny of *Caenorhabditis* reveals frequent loss of introns during nematode evolution. Genome Res 14, 1207–1220.

Cohen, F.E., Sternberg, M.J., 1980. On the use of chemically derived distance constraints in the prediction of protein structure with myoglobin as an example. J. Mol. Biol. 137, 9–22.

Conradt, B., Wu, Y.C., Xue, D., 2016. Programmed cell death during *Caenorhabditis elegans* development. Genetics 203, 1533–1562.

Coroian, C., Broitman-Maduro, G., Maduro, M.F., 2006. Med-type GATA factors and the evolution of mesendoderm specification in nematodes. Dev. Biol. 289, 444–455.

Cutter, A.D., 2008. Divergence times in *Caenorhabditis* and *Drosophila* inferred from direct estimates of the neutral mutation rate. Mol. Biol. Evol. 25, 778–786.

Cutter, A.D., Felix, M.A., Barriere, A., Charlesworth, D., 2006. Patterns of nucleotide polymorphism distinguish temperate and tropical wild isolates of *Caenorhabditis briggsae*. Genetics 173, 2021–2031.

Deppe, U., Schierenberg, E., Cole, T., Krieg, C., Schmitt, D., Yoder, B., von Ehrenstein, G., 1978. Cell lineages of the embryo of the nematode *Caenorhabditis elegans*. Proc. Natl. Acad. Sci. USA 75, 376–380.

Dolgin, E.S., Felix, M.A., Cutter, A.D., 2008. Hakuna Nematoda: genetic and phenotypic diversity in African isolates of *Caenorhabditis elegans* and *C. briggsae*. Heredity 100, 304–315.

Felix, M.A., Duveau, F., 2012. Population dynamics and habitat sharing of natural populations of *Caenorhabditis elegans* and *C. briggsae*. BMC Biol. 10, 59.

Fierst, J.L., Willis, J.H., Thomas, C.G., Wang, W., Reynolds, R.M., Ahearne, T.E., Cutter, A.D., Phillips, P.C., 2015. Reproductive mode and the evolution of genome size and structure in *Caenorhabditis* nematodes. PLoS Genet 11, e1005323.

Fodor, A., Riddle, D.L., Nelson, F.K., Golden, J.W., 1983. Comparison of a new wild-type *Caenorhabditis briggsae* with laboratory strains of *C. briggsae* and *C. elegans*. Nematologica 29, 203–217.

Fraser, A.G., Kamath, R.S., Zipperlen, P., Martinez-Campos, M., Sohrmann, M., Ahringer, J., 2000. Functional genomic analysis of *C. elegans* chromosome I by systematic RNA interference. Nature 408, 325–330.

Gönczy, P., Echeverri, C., Oegema, K., Coulson, A., Jones, S.J., Copley, R.R., Duperon, J., Oegema, J., Brehm, M., Cassin, E., Hannak, E., Kirkham, M., Pichler, S., Flohrs, K., Goessen, A., Leidel, S., Alleaume, A.M., Martin, C., Ozlu, N., Bork, P., Hyman, A.A., 2000. Functional genomic analysis of cell division in *C. elegans* using RNAi of genes on chromosome III. Nature 408, 331–336.

Gupta, B.P., Sternberg, P.W., 2003. The draft genome sequence of the nematode *Caenorhabditis briggsae*, a companion to *C. elegans*. Genome Biol. 4, 238.

Hillier, L.W., Miller, R.D., Baird, S.E., Chinwalla, A., Fulton, L.A., Koboldt, D.C., Waterston, R.H., 2007. Comparison of *C. elegans* and *C. briggsae* genome sequences reveals extensive conservation of chromosome organization and synteny. PLoS Biol. 5, e167.

Hoeppner, D.J., Hengartner, M.O., Schnabel, R., 2001. Engulfment genes cooperate with *ced-3* to promote cell death in *Caenorhabditis elegans*. Nature 412, 202–206.

Horvitz, H.R., 2003. Worms, life, and death (Nobel lecture). Chembiochem. Eur. J. Chem. Biol. 4, 697–711.

Houthoofd, W., Jacobsen, K., Mertens, C., Vangestel, S., Coomans, A., Borgonie, G., 2003. Embryonic cell lineage of the marine nematode *Pellioditis marina*. Dev. Biol. 258, 57–69.

Hutter, H., Schnabel, R., 1994. *glp-1* and inductions establishing embryonic axes in *C. elegans*. Development 120, 2051–2064.

Hutter, H., Schnabel, R., 1995a. Establishment of left-right asymmetry in the *Caenorhabditis elegans* embryo: a multistep process involving a series of inductive events. Development 121, 3417–3424.

Hutter, H., Schnabel, R., 1995b. Specification of anterior-posterior differences within the AB lineage in the *C. elegans* embryo: a polarising induction. Development 121, 1559–1568.

Kaletta, T., Schnabel, H., Schnabel, R., 1997. Binary specification of the embryonic lineage in *Caenorhabditis elegans*. Nature 390, 294–298.

Kamath, R.S., Fraser, A.G., Dong, Y., Poulin, G., Durbin, R., Gotta, M., Kanapin, A., Le Bot, N., Moreno, S., Sohrmann, M., Welchman, D.P., Zipperlen, P., Ahringer, J., 2003. Systematic functional analysis of the *Caenorhabditis elegans* genome using RNAi. Nature 421, 231–237.

Kemphues, K.J., Priess, J.R., Morton, D.G., Cheng, N.S., 1988. Identification of genes required for cytoplasmic localization in early *C. elegans* embryos. Cell 52, 311–320.

Kiontke, K., Fitch, D.H., 2005. The phylogenetic relationships of *Caenorhabditis* and other rhabditids. WormBook, 1–11.

Kiontke, K., Sudhaus, W., 2006. Ecology of *Caenorhabditis* speciesWormBook, 1–14.

Kiontke, K., Gavin, N.P., Raynes, Y., Roehrig, C., Piano, F., Fitch, D.H., 2004. *Caenorhabditis* phylogeny predicts convergence of hermaphroditism and extensive intron loss. Proc. Natl. Acad. Sci. USA 101, 9003–9008.

Lee, J.Y., Goldstein, B., 2003. Mechanisms of cell positioning during *C. elegans* gastrulation. Development 130, 307–320.

Maduro, M.F., Kasmir, J.J., Zhu, J., Rothman, J.H., 2005. The Wnt effector POP-1 and the PAL-1/Caudal homeoprotein collaborate with SKN-1 to activate *C. elegans* endoderm development. Dev. Biol. 285, 510–523.

Mango, S.E., Lambie, E.J., Kimble, J., 1994. The *pha-4* gene is required to generate the pharyngeal primordium of *Caenorhabditis elegans*. Development 120, 3019–3031.

McDiarmid, T.A., Au, V., Loewen, A.D., Liang, J., Mizumoto, K., Moerman, D.G., Rankin, C.H., 2018. CRISPR-Cas9 human gene replacement and phenomic characterization in *Caenorhabditis elegans* to understand the functional conservation of human genes and decipher variants of uncertain significance. Dis. Model Mech..

Nance, J., 2005. PAR proteins and the establishment of cell polarity during *C. elegans* development. BioEssays: News Rev. Mol. Cell. Dev. Biol. 27, 126–135.

Nance, J., Priess, J.R., 2002. Cell polarity and gastrulation in *C. elegans*. Development 129, 387–397.

Okamoto, H., Thomson, J.N., 1985. Monoclonal antibodies which distinguish certain classes of neuronal and supporting cells in the nervous tissue of the nematode *Caenorhabditis elegans*. J. Neurosci. 5, 643–653.

Owraghi, M., Broitman-Maduro, G., Luu, T., Roberson, H., Maduro, M.F., 2010. Roles of the Wnt effector POP-1/TCF in the *C. elegans* endomesoderm specification gene network. Dev. Biol. 340, 209–221.

Park, F.D., Priess, J.R., 2003. Establishment of POP-1 asymmetry in early *C. elegans* embryos. Development 130, 3547–3556.

Priess, J.R., Thomson, J.N., 1987. Cellular interactions in early *C. elegans* embryos. Cell 48, 241–250.

Priess, J.R., Schnabel, H., Schnabel, R., 1987. The *glp-1* locus and cellular interactions in early *C. elegans* embryos. Cell 51, 601–611.

Reymann, A.C., Staniscia, F., Erzberger, A., Salbreux, G., Grill, S.W., 2016. Cortical flow aligns actin filaments to form a furrow. Elife, 5.

Rocheleau, C.E., Downs, W.D., Lin, R., Wittmann, C., Bei, Y., Cha, Y.H., Ali, M., Priess, J.R., Mello, C.C., 1997. Wnt signaling and an APC-related gene specify endoderm in early *C. elegans* embryos. Cell 90, 707–716.

Schierenberg, E., 1987. Reversal of cellular polarity and early cell-cell interaction in the embryos of *Caenorhabditis elegans*. Dev. Biol. 122, 452–463.
Schnabel, R., 1991. Cellular interactions involved in the determination of the early *C. elegans* embryo. Mech. Dev. 34, 85–99.
Schnabel, R., Priess, J.R., 1997b. Specification of cell fates in the early Embryo. In: Riddle, D.L., Blumenthal, T., Meyer, B.J., Priess, J.R. (Eds.), C. elegans II. Cold Spring Harbor, NY.
Schnabel, R., Hutter, H., Moerman, D., Schnabel, H., 1997a. Assessing normal embryogenesis in *Caenorhabditis elegans* using a 4D microscope: variability of development and regional specification. Dev. Biol. 184, 234–265.
Schnabel, R., Bischoff, M., Hintze, A., Schulz, A.K., Hejnol, A., Meinhardt, H., Hutter, H., 2006. Global cell sorting in the *C. elegans* embryo defines a new mechanism for pattern formation. Dev. Biol. 294, 418–431.
Schneider, S.Q., Bowerman, B., 2003. Cell polarity and the cytoskeleton in the *Caenorhabditis elegans* zygote. Annu Rev. Genet. 37, 221–249.
Schulze, J., Schierenberg, E., 2011. Evolution of embryonic development in nematodes. Evodevo 2, 18.
Shaye, D.D., Greenwald, I., 2011. OrthoList: a compendium of *C. elegans* genes with human orthologs. PLoS One 6, e20085.
Sonnichsen, B., Koski, L.B., Walsh, A., Marschall, P., Neumann, B., Brehm, M., Alleaume, A.M., Artelt, J., Bettencourt, P., Cassin, E., Hewitson, M., Holz, C., Khan, M., Lazik, S., Martin, C., Nitzsche, B., Ruer, M., Stamford, J., Winzi, M., Heinkel, R., Roder, M., Finell, J., Hantsch, H., Jones, S.J., Jones, M., Piano, F., Gunsalus, K.C., Oegema, K., Gönczy, P., Coulson, A., Hyman, A.A., Echeverri, C.J., 2005. Full-genome RNAi profiling of early embryogenesis in *Caenorhabditis elegans*. Nature 434, 462–469.
Stein, L.D., Bao, Z., Blasiar, D., Blumenthal, T., Brent, M.R., Chen, N., Chinwalla, A., Clarke, L., Clee, C., Coghlan, A., Coulson, A., D'Eustachio, P., Fitch, D.H., Fulton, L.A., Fulton, R.E., Griffiths-Jones, S., Harris, T.W., Hillier, L.W., Kamath, R., Kuwabara, P.E., Mardis, E.R., Marra, M.A., Miner, T.L., Minx, P., Mullikin, J.C., Plumb, R.W., Rogers, J., Schein, J.E., Sohrmann, M., Spieth, J., Stajich, J.E., Wei, C., Willey, D., Wilson, R.K., Durbin, R., Waterston, R.H., 2003. The genome sequence of *Caenorhabditis briggsae*: a platform for comparative genomics. PLoS Biol. 1, E45.
Sudhaus, W., 1974. Zur Systematik, Verbreitung, Okologie und Biologie neuer und wenig bekannter Rhabditiden (Nematoda) 2. Teil.
Sulston, J.E., 1983. Neuronal cell lineages in the nematode *Caenorhabditis elegans*. Cold Spring Harb. Symp. Quant. Biol. 48 (Pt 2), 443–452.
Sulston, J.E., Horvitz, H.R., 1977. Post-embryonic cell lineages of the nematode, *Caenorhabditis elegans*. Dev. Biol. 56, 110–156.
Sulston, J.E., White, J.G., 1980. Regulation and cell autonomy during postembryonic development of *Caenorhabditis elegans*. Dev. Biol. 78, 577–597.
Sulston, J.E., Schierenberg, E., White, J.G., Thomson, J.N., 1983. The embryonic cell lineage of the nematode *Caenorhabditis elegans*. Dev. Biol. 100, 64–119.
Thorpe, C.J., Schlesinger, A., Carter, J.C., Bowerman, B., 1997. Wnt signaling polarizes an early *C. elegans* blastomere to distinguish endoderm from mesoderm. Cell 90, 695–705.
True, J.R., Haag, E.S., 2001. Developmental system drift and flexibility in evolutionary trajectories. Evol. Dev. 3, 109–119.
Vermeij, G.J., 2015. Forbidden phenotypes and the limits of evolution. Interface Focus 5, 20150028.
Verster, A.J., Ramani, A.K., McKay, S.J., Fraser, A.G., 2014. Comparative RNAi screens in *C. elegans* and *C. briggsae* reveal the impact of developmental system drift on gene function. PLoS Genet 10, e1004077.
Wood, W.B., 1988. Determination of pattern and fate in early embryos of *Caenorhabditis elegans*. Dev. Biol., 57–78.
Wood, W.B., Kershaw, D., 1991. Handed asymmetry, handedness reversal and mechanisms of cell fate determination in nematode embryos. Ciba Found. Symp 162, 143–159, (discussion 159-164).
Zhao, Z., Boyle, T.J., Bao, Z., Murray, J.I., Mericle, B., Waterston, R.H., 2008. Comparative analysis of embryonic cell lineage between *Caenorhabditis briggsae* and *Caenorhabditis elegans*. Dev. Biol. 314, 93–99.
zur Strassen, O., 1959. Neue Beiträge zur Entwicklungsmechanik der Nematoden. Zoologica 107, 1–142.